A Mechanistic and Kinetic Investigation of a Cobalt-Catalyzed Heterodimerization of Acrylates and 1,3-Dienes. Reaction Progress Analysis and a Potential Role of Cationic Cobalt(I) Intermediates

Undergraduate Research Thesis

Presented in Partial Fulfillment of the Requirements for graduation *with Research Distinction* in Chemistry in the undergraduate colleges of The Ohio State University

By: Montgomery Gray

The Ohio State University

15th December 2019

Project Advisors: Dr. T.V. RajanBabu and Nicholas Brunelli

Abstract

Very few process that directly couple alkenes and other feedstock materials are used in industry, with the exceptions being dimersol technology (propene dimerization), Shell Higher Olefin Process, and acrylonitrile dimerization. This is in part because of the low turnover number (TON) achieved by these processes, even though high regio- and enantioselectivies can be achieved. Using in situ IR spectroscopy to monitor a cobalt catalyzed heterodimerization between an acrylate and diene reaction progress kinetic analysis (RPKA) was carried out. This along with the isolation and characterization of low-valent cobalt catalyst precursors, many important mechanistic details were discovered. (i) The reaction possesses an induction period that requires two hours of stir time to generate the active catalyst. (ii) The time it takes for the reduction of Co(II) to Co(I) and then to $[Co(I)]^+$ are the primary reason for the observed induction period. (iii) RPKA using in situ IR spectroscopy, the same excess experiments showed that the active catalyst concentration stays consistent throughout the reaction and low TON is due to the instability of the active $[Co(I)]^+$ species. (iv) Different excess experiments show that the reaction is first order in the diene and zeroth order in the acrylate (confirmed by VTNA). (v) Through variation in catalyst loading, it is revealed that the reaction is first order in the catalyst (confirmed by VTNA). (vi) An oxidative addition/reduction elimination through Co(I)/Co(III) mechanism is proposed. Based on the mechanistic findings, the TON of the reaction was increased by a factor of 10 through increasing the initial concentration of the starting materials, specifically the diene, which is able to stabilize the active catalytic species. Isolation and characterization of an inactive tetra-ligated cationic Co(I) species suggest that the formation of this species is a possible pathway of deactivation of the catalyst.

Acknowledgements

I would firstly like to thank Dr. RajanBabu for introducing me to the amazing world that is organic chemistry. It was his undergraduate organic chemistry course that encouraged me to start my journey in organic chemistry and for that I will always be grateful. I would also like to thank Dr. RajanBabu for always showing a passion for science and chemistry in particular. Your love for chemistry was contagious and made coming into lab and group meeting something to always look forward to.

I would also like to thank Dr. Nicholas Brunelli for being one of two great academic mentors who always pushed me to do my best. My undergraduate research experience would not have been nearly as meaningful as it was without your guidance and mentorship.

Perhaps most importantly I would like to thank Michael Hines, my partner in this research. He stuck with me throughout the entire project even when things were not going well. I could not have produced such fine work without his chemical engineering and MATLAB expertise.

I would also like to thank the graduate students and postdocs of the RajanBabu lab, Mahesh Parsutkar, James Herbort, Dr. Srinivasarao Tenneti, Dr. Vinayak Pager, Dr. Stanley Jing, Dr. Krishnaja Duvvuri, Milauni Mehta, and Jon Gordon, for answering my endless amount of questions and teaching me what it means to be a chemist. You guys all made coming in to lab super fun! I have learned more than I could have ever hoped to!

Lastly I would like to thank my mother and father for instilling on me the importance of education and trying ones hardest! Thank you for being such wonderful parents and always hoping for the best for me! I would not be the person I am today without all you.

Table of Contents

Table of Contents

List of Tables

List of Figures

List of Abbreviations

α	alpha
β	beta
NaBArF	sodium *tetrakis*[bis-(3,5-trifluoromethyl) phenyl] borate
°C	degrees centigrade/Celsius
δ	chemical shift in parts per million
d	doublet (NMR)
DCM	dichloromethane
dd	doublet of doublets (NMR)
DPPP	1,3-bis(diphenylphosphino)propane
dpppent	1,5-bis(diphenylphosphino)pentane
dt	doublet of triplets (NMR)
ee	enantiomeric excess
equiv/eq	equivalent
g	gram
GC	gas chromatography
h	hour
η	eta
λ	lambda
min	minute
mol	moles
NMR	nuclear magnetic resonance
q	quartet (NMR)

RPKA	Reactrion Progress Kinetic Analysis
rt	room temperature
s	singlet (NMR)
t	triplet (NMR)
temp	temperature
THF	tetrahydrofuran
UV-Vis	ultraviolet and visible light

Chapter 1: Introduction and Background

The creation and development of selective catalyst for the coupling of feedstock chemicals can have large impacts on the manufacture, synthesis and design of molecules that hold interest in for materials and medicine.[1] Some of the most used chemicals in industry are alkenes (such as 1,3-dienes) and acrylates, however, their use in direct coupling reactions is not common.[2] Instead, dienes and acrylates are typically used as monomers[3] because their direct coupling is dampened by the use of expensive catalyst and their resulting turnover number (TON) are low. The key challenge in increasing the relevance (TON) of direct heterodimerization between acrylates and dienes is the limited understanding of their mechanism and the chemical driving forces that enable this transformation. Recent work on heterodimerizations between 1,3-dienes and alkyl acrylates has looked at catalytic systems that give high stereo- and regioselectivity, but with low TONs (on the order of 200). Through better understanding of the mechanism for this reaction, it is hoepd that both the yield and the TON can be improved. Through understanding the kinetics of this reaction a better mechanistic understanding would be achieved, and the kinetics could be used to enhance the performance of the catalyst (selectivity, TON, rates, and yield).

Heterodimerization reactions have been intensely studied with some of the more important examples being Rh-catalyzed 1,3-butadiene-ethylene dimerization, which has been examined in regards to the synthesis of 1,4-hexadiene, a monomer for elastomers.[4] Another related reaction is the dimerization between 1,3-butadiene and methyl acrylate, this reaction first appearing in 1964.[5] However, this reaction has never seen full development into commercial use (Eq 1).

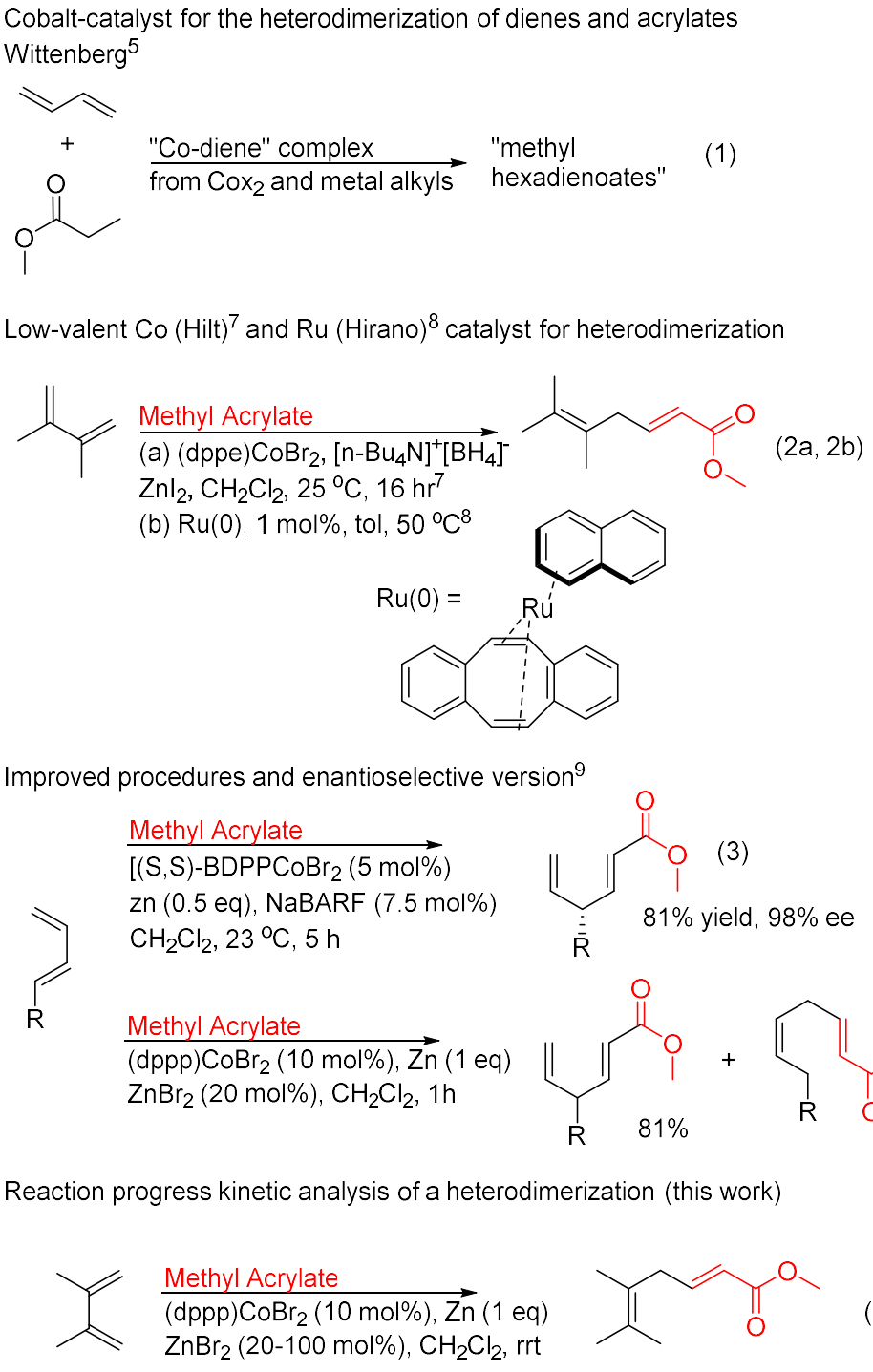

Figure 1. Evolution of heterodimerization reactions.

Until recently, different kind of dienes and acrylates that can be used in these heterodimerization reactions was very limited. The selectivity's also had room for improvement.[6-

[9] In 2001, Hilt et al reported one of the first cobalt catalyzed heterodimerization reactions between 2,3-dimethyl-1,3-butadiene and t-butyl acrylate (eq 2a).[7] A more recent example of similar chemistry was performed by Hirano et al. In this report a Ru(0) complex was able to codimerize alkyl acrylates and 1,3-dienes (eq 2b).[8] In 2017, the RajaBabu group described an enantioselective version of this reaction (the first time an enantioselective version was reported). The chiral cationic cobalt(I)-*bis*-phosphine complexes such as [(*S,S*)-BDPP]Co]$^+$ X$^-$ [BDPP = 2,4-*bis*(diphenylphosphino)pentane; X = [3,5-$(CF_3)_2C_6H_3]_4B^-$), abbreviated as $BArF^-$] was shown to have a broad scope, give excellent %ee, and give excellent selectivities (Eq 3). While these studies were being performed it was also found that making small changes to the Hilt procedure[7b] using [1,3-*bis*-(diphenylphosphino)propane)]$CoBr_2$ allowed for an alternative the codimerization of 1,3-dienes and acrylates (Eq 4).[10] Because of the inexpensive and abundant nature of these reagents and starting materials and the fact that they can be coupled with high selectivities, it seems that they could provide an inexpensive route to value added intermediates.

Because these methods allow for the heterodimerization of 1,3-dienes and acrylates using an inexpensive cobalt catalyst, this system could be very valuable industrially if higher values for TON can be achieved. Through analysis of many dimerization catalyst, it has been suggested that low-valent cobalt species formed in situ from *bis*-diarylphosphinoalkane-cobalt(II) salts posses the largest potential for these type of reactions. However, not much is known about the mechanisms that these type of reactions proceed through.

In principle, the cobalt catalyzed heterodimerization has two general mechanisms that it could go through (Figure 2), both of which have been suggested for olefin dimerization reactions.[2a] (A) one involves the formation of discrete metal-hydrides and goes through no change in oxidation state of the metal throughout the catalytic cycle (commonly invoked in nickel catalyzed

reactions)[11], and (B) an oxidative dimerization that has the metal undergo redox changes. Such a mechanism is proposed in dimerization reactions that are catalyzed by Co[9,12] and Ru[13]. Determining which mechanistic cycle is followed has the possibility to provide insight that would allow this reaction to be performed at high TON while also using an inexpensive catalyst.

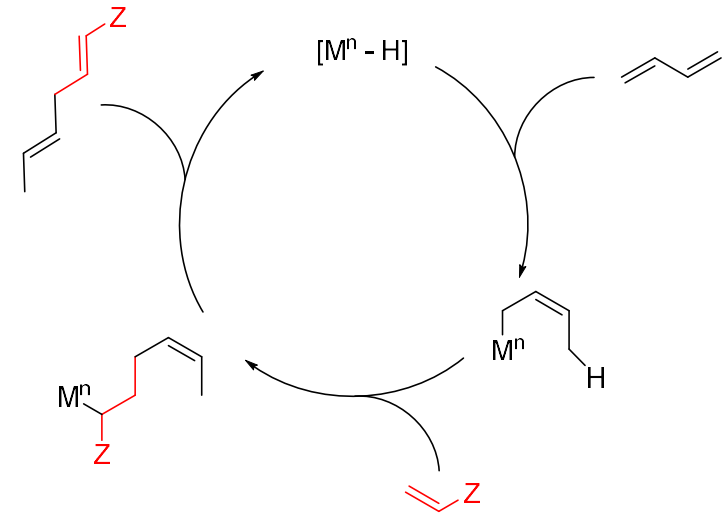

A. Hydride route to dimerization

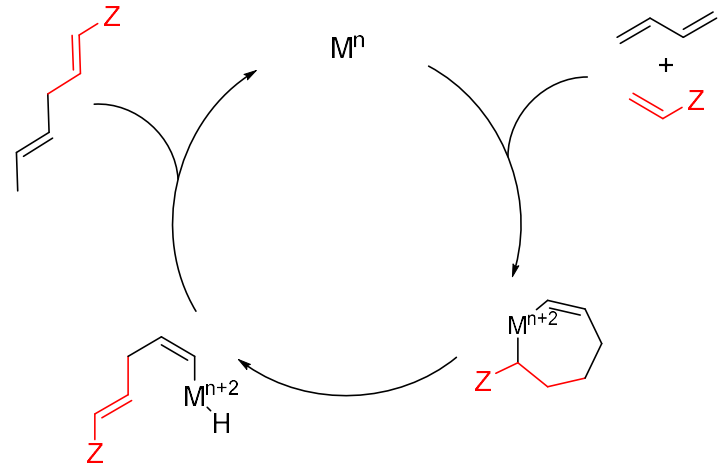

B. Oxidative coupling route to dimerization

Figure 2. Two possible mechanisms for cobalt catalyzed heterodimerization reactions.

Using traditional methods such as pseudo-first order, where one of the substrates is made to have a high concentration compared to the other, could be used to investigate the kinetics of this reaction, it has been recognized that unusually high concentrations of one substrate have the possibility to change the reactions mechanism. In actuality, using concentrations that closely resemble that of the actual reaction conditions allow for the most accurate kinetics and mechanistic insights to be obtained. This is true because high concentrations may cause competitive binding of substrates that may alter the observed reaction mechanism. Using in situ measurements and reaction progress kinetic analysis (RPKA) it is possible to use the actual substrate concentrations when studying the reactions kinetics and mechanism.[14] For heterodimerization chemistry, the in situ monitoring offers many advantages over traditional methods, since the catalyst is sensitive to both moisture and oxygen. This avoids tracking the reaction through small aliquots that could introduce minute amounts of oxygen or moisture. Additionally, in situ measurements (using IR spectroscopy) allows for continuous monitoring of the reactants concentrations.

In this work, an RPKA[14] approach using in situ IR spectroscopy is used to study a prototypical diene-acrylate dimerization between methyl acrylate and 2,3-dimethylbutadiene (Figure 1, Eq 5) with the goal of providing further details on the mechanism of an important class of reactions exemplified by this transformation. The initial experiments showed the presence of an induction period. The induction period was attributed to the pre-catalyst (Co(II)) was transformed into the active catalyst ($[Co(I)]^+$). The nature of this catalyst was clarified using UV-Visible spectroscopy along with isolation of the relevant intermediates that were deemed responsible for the catalysis. Through the use of a consistent stirring period, experiments were performed that were able to investigate the reaction order of the diene, acrylate, and catalyst in a reproducible fashion. The results from these experiments were used to propose a potential reason that low TON

are obtained from this reaction. Using this information, the reaction conditions were modified which allowed for the TON to be increased by an order of magnitude.

Chapter 2: Kinetic and Mechanistic Investigation of a Cobalt Mediated Heterodimerization

2.1 Catalyst Activation.

Using a standard probe reaction of 2,3-dimethyl-1,3-butadiene and methyl acrylate under the conditions described in equation 6, the cobalt catalyzed heterodimerization reaction was investigated. The general procedure involves the combining of (DPPP)$CoBr_2$ (ranging 10-25 mol%), Zn (1 eq), and $ZnBr_2$ under a nitrogen atmosphere in 2 mL of dichloroethane (DCE) at 30 ^oC. Once the above reagents were combined, the flask was equipped with a ReactIR probe, after which, the reaction was started by the addition of both 2,3-dimethyl-1,2-butadiene (1 eq) and methyl acrylate (ranging 1.1-2.4 eq) in 2 mL DCE. Once the two starting materials were added, several new peaks in the FT-IR spectrum were seen. From background experiments, it was shown that the peak at 896 cm^{-1} (=CH_2 out-of-plane wagging)[15a] and 1401 cm^{-1} (scissoring of the terminal methylene)[15b] were from the diene and acrylate respectively. Both the 896 cm^{-1} and the 1401 cm^{-1} peaks are well separated from others and because of this could reliably be used to quantify the amount of each substrate in the reaction mixture as the reaction progressed. By extracting these two intensities over time, it was seen that the concentration of the two substrates decreases over time, as can be seen in Figure 4.

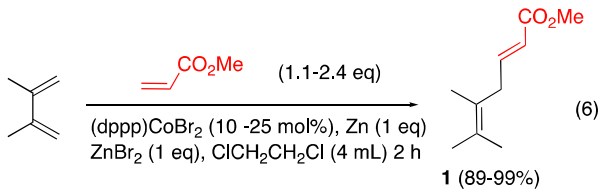

Figure 3. Generic reaction scheme followed throughout the experiments.

Early in the experimentation process, it was found that the reaction gives an induction period. This was found by performing the reaction using different catalyst activation times before

the addition of the diene and acrylate. Upon using an activation time of five minutes, the concentration of the substrates initially decreased slowly followed by a faster reaction rate. This behavior suggest that the catalyst that performs the reaction was not present in high concentrations in the beginning of the reaction. Not only this, but it was found that using a five minute stir time also provided data that was hard to reproduce. This irreproducibility is attributed to the fact that the catalyst was not all the way formed (i.e., reduction of Co(II) to a Co(I) species and, possibly, subsequent formation of a cationic species (see later for details) likely caused by the use of insoluble reagents, including metallic Zn.

To obtain kinetics that were reproducible, several experiments were performed that changed the stir time systematically by allowing the (DPPP)$CoBr_2$, Zn, and $ZnBr_2$ to stir for different amounts of time in DCE before adding in the diene and acrylate. In Figure 4, the different stir times that were performed can be seen. When compared to the five minute stir times, longer stir times gave more reproducible data. The data when performing a stir time of one hour still possessed an initial period of slow conversion followed by an acceleration in reaction rate (induction period), this suggested that the catalyst was still being activated. It was found that a stir time of two hours provided reproducible reaction profiles that were consistant with first order kinetics. Stir times that were longer than two hours gave similar results. Thus, a two hour stir time was used for all preceding kinetic and mechanistic investigations in this work.

2.2 Induction period and UV spectroscopy.

The presence of an induction period suggest that (DPPP)$CoBr_2$ is a pre-catalyst that is subsequently transformed into the active catalyst when in the presence of a reducing agent (Zn) and an activator ($ZnBr_2$). The presence of an induction period promoted an investigation of other possible cobalt species that were present in the solution using UV-Vis spectroscopy (Figure 5).

UV-Vis spectroscopy was used to characterize and differentiate different cobalt species that were proposed to be present in the catalytic cycle, this includes: (DPPP)$Co^{(II)}Br_2$, '(DPPP)$Co^{(I)}$Br', and '[(DPPP)$Co^{(I)}$]$^{+}$' [DPPP = 1,3-Bis-(diphenyl phosphino) propane].[16] The activation conditions that were used for the reactions were simulated by stirring (DPPP)$CoBr_2$, Zn, and $ZnBr_2$ in DCE for two hours with rigorous exclusion of oxygen at the concentrations that the reactions are typically performed [0.0155-0.0375 M of (DPPP)$CoBr_2$]. The excess undissolved Zn was filtered off and the supernatant solution was then used for the UV-Vis measurements. In order to obtain the UV-Vis spectra, the sample was further diluted using DCE in order to avoid excessive absorption in the spectral region of interest

Three distinct peaks above the wavelength of 400 nm were seen in the UV-Vis spectrum of (DPPP)$Co^{(II)}Br_2$, the peaks were 633 nm, 662 nm, and 735 nm (Figure 5). This spectrum was consistent with previous characterizations of Co(II) complexes like $X_2Co(PPh_3)_2$ [e.g., 605 nm, 635 nm and 745 nm for $Cl_2Co(PPh_3)_2$ in benzene[17a] or 591, 636 and 728 for (DPPP)$CoCl_2$ in CH_2Cl_2[17c] (Table 1)]. Significantly, The Co(II) complex had no peaks around 500 nm and 900 nm that would be characteristic of Co(I) compounds. A similar Co(I) species $((PH_3P)_3CoCl$ was reported to have absorptions at 745 and 940 nm in benzene (run in the presence of excess ligand to avoid decomposition) in addition to peaks at 605 nm and 635 nm ascribed to Co(II) species formed in situ by slow disproportionation of Co(I) species to Co(II) and metallic Co.[17a, 17c] In addition, a bromo-derivative $(Ph_3P)_3CoBr$ had peaks at 750 nm and 970 nm.[17b]

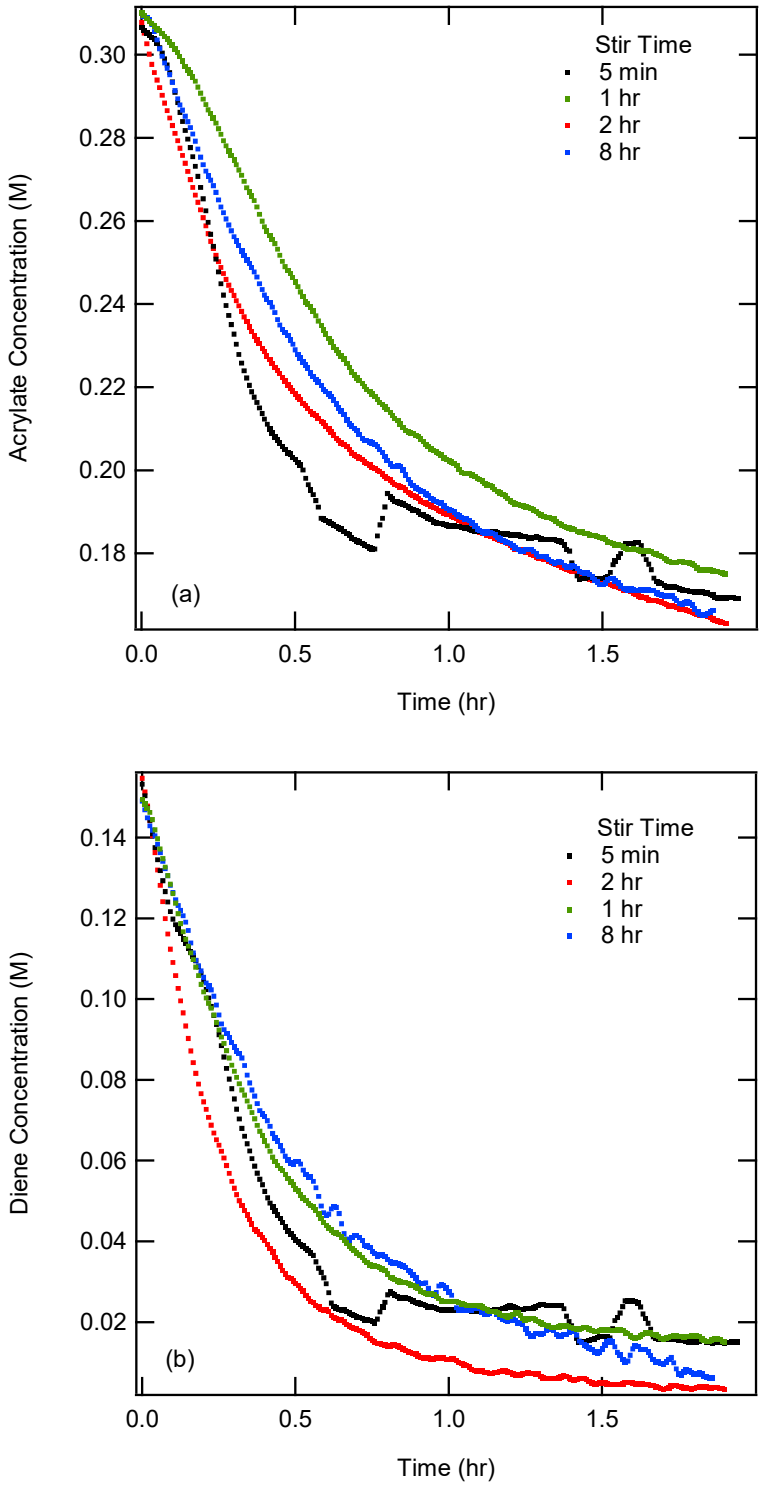

Figure 4. (a) Acrylate concentration, measured by the intensity at 1401 cm^{-1}, vs time for stir time investigations at 5 min, 1 hour, 2 hours, and 8 hours. (b) Diene concentration, measured by the intensity at 896 cm^{-1}, vs. time for stir time investigations at 5 min, 1 hour, 2 hours, and 8 hours.

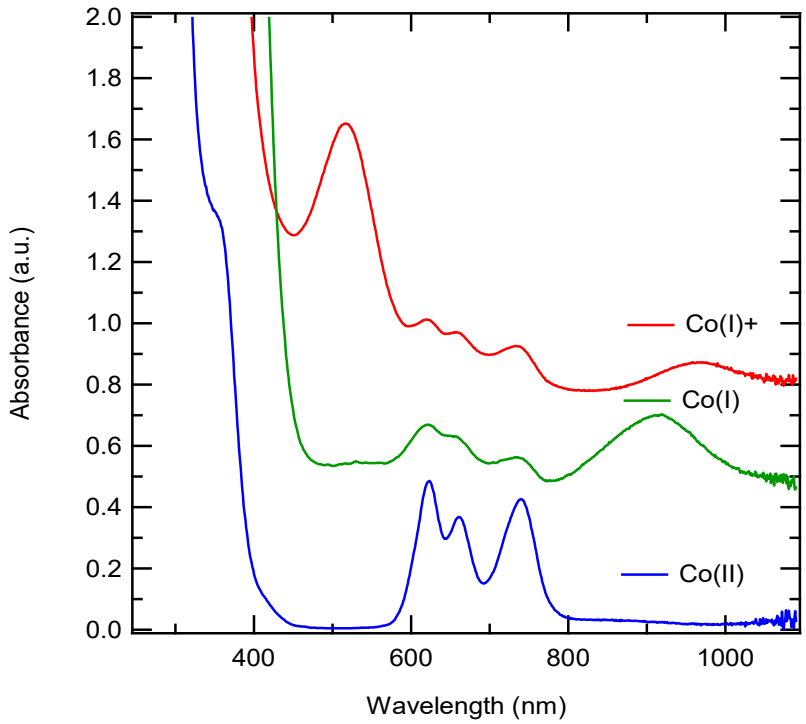

Figure 5. UV-Vis spectra of (DPPP)Co(II)Br_2 (Blue), $(DPPP)_3Co_2(I)Br_2$ (3, Green), and $[(DPPP)Co(I)]^+$ (Red) in dichloroethane. (DPPP)Co(II)Br_2 (Blue) and $(DPPP)_3Co_2(I)Br_2$ (3, Green) were obtained from pure crystallized materials of the named compound. $[(DPPP)Co(I)]^+$ (Red) was obtained by the following: the supernatant of a reaction mixture of (DPPP)Co(II)Br_2, Zn, and $ZnBr_2$ that was stirred for two hours in a glovebox.

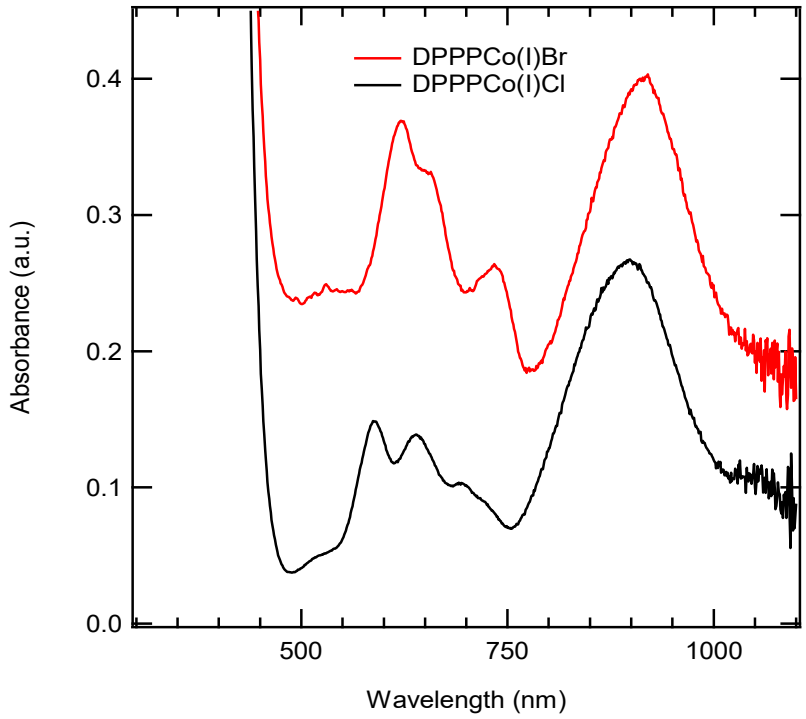

Figure 6. UV-Vis spectra of $(DPPP)_3Co_2Cl_2$ (2, black) and $(DPPP)_3Co_2Br_2$ (3, red). See Table 1 for structures.

Model Co(I) complexes were prepared (the two complexes prepared, 2 and 3 can be seen in Table 1). These two complexes were fully characterized via X-ray crystallography.[18] The UV-Vis spectra for these two complexes were recorded in DCE, the corresponding UV-Vis spectra can be seen in Figure 6. The chloro-compound shows major peaks at 510 nm, 710 nm, and 910 nm and the analogous bromo-compound has peaks at 510 nm, 725 nm, and 935 nm (additionally, two broad absorptions can be seen at ca. 600 nm. This is most likely due to contamination from the corresponding Co(II) species that arose from the previously mentioned disproportionation reactions). These absorptions match those from the authentic Co(I) complexes reported in the literatures (see for example, of $(Ph_3P)_3CoCl$ and $(Ph_3P)_3CoBr$), See Table 1.[17a-b] After storage of these compounds or exposing them to oxygen, the peaks that are associated with the Co(I) species quickly disappear, this is reported for other Co(I) complexes such as $(Ph_3P)_3CoBr$ (Figure 7).

Stirring a mixture of $(DPPP)CoBr_2$, Zn and $ZnBr_2$ and following the UV absorptions of the supernatant (Figure 8) provided insight into the induction period. Because both Co(I) and Co(II) absorb strongly in the UV-Vis region, the concentration of the pre-catalyst, reducing agent, and activator were made lower than the typical experiment, affecting the time for the catalyst to be activated. As time progressed, the peaks that were characteristic for Co(I) at 740 nm and the broad peak at 900 nm increased until a maximum was reached at 240 minutes (Figure 8). Parallel behavior was observed for the strong peak at 517 nm, which also reached it maximum intensity at ca. 240 minutes. No further changes were observed in the spectrum after this time period. The peak at 517 nm was assigned to the active catalyst, $(DPPP)Co(I)^+$.[16] Further support for such a claim also came from NMR studies. While as expected ^{31}P NMR of $(DPPP)CoBr_2$ in $CDCl_3$ shows no signals, addition of excess Zn and mixing for 15 minutes gave two signals at δ -21.87 and 15.47 in an approximate ratio of 2:1 respectively. Further addition of $ZnBr_2$ (2 eq with respect to Co(II)-

complex) after 30 minutes only one peak at δ -21.89 was observed. This peak is believed to correspond to the catalytically competent $[LCo^{(I)}]^+$ species. A similar species was produced when $(DPPP)CoBr_2$ is reduced with zinc in the presence of NaBArF.

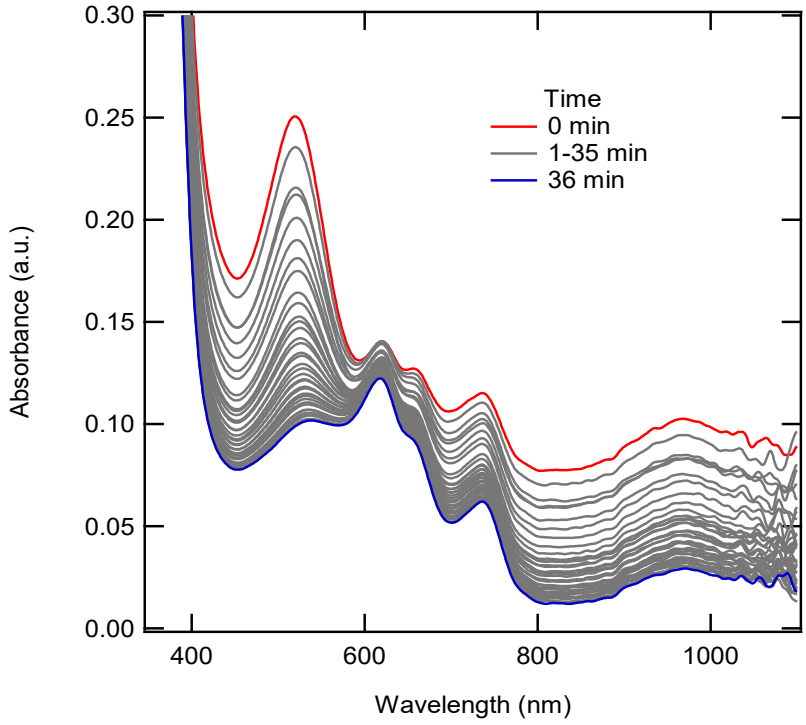

Figure 7. The supernatant of a reaction mixture of $(DPPP)Co(II)Br_2$, Zn, and $ZnBr_2$ was mixed for two hours. After removing the excess Zn, the solution was allowed to sit at room temperature. The UV-Vis spectrum was recorded from 0 to 36 minutes. The plots shown are smoothed. The initial intensity (0 minutes) is shown red with the final intensity (36 minutes) is shown in blue, all intermediate intensities are gray.

Table 1. UV-Visible Spectra of Cobalt(I) and Cobalt(II) Complexes

Compound	$(Ph_2P)CoCl_2$	$(dppp)CoBr_2$	$[Ph_3P]_3CoCl$	$[Ph_3P]_3CoBr$
λ_{max} (nm)	(605, 635, 745)	(622,662,735)	(745, 970)	(750, 970)
Compound	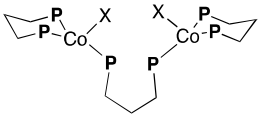 Co(I): $(dppp)_3Co_2X_2$		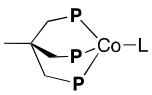 Co(I)	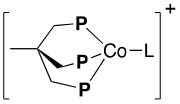 [Co(I)]+
λ_{max} (nm)	2 X = Cl (710, 910)	3 X = Br (725, 935) 3 + NaBARF (500, 970)	4 L = Cl (530, 826)	5 L = η^4-1,3-butadiene (460)

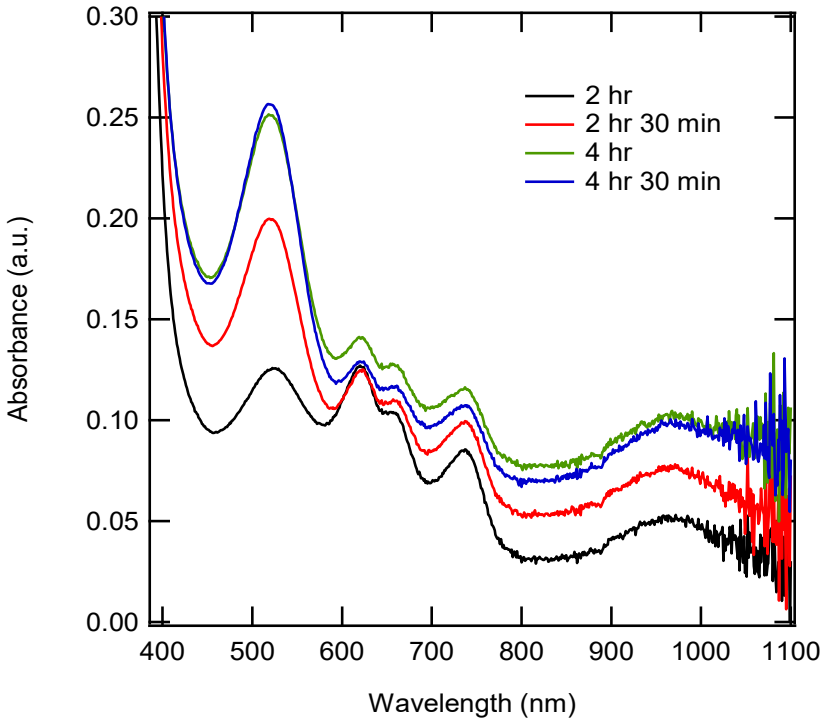

Figure 8. The supernatant of a reaction mixture of (DPPP)Co(II)Br_2, Zn, and $ZnBr_2$ was mixed for different amounts of time. The peak at 517 nm stopped increasing at about four hours and thirty minutes.

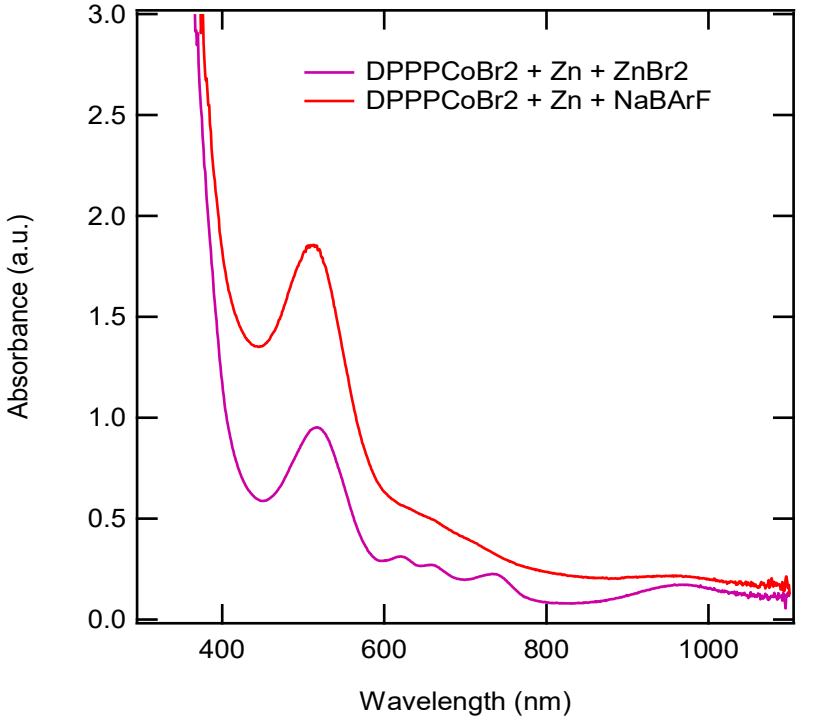

Figure 9. Zn-Reduced DPPPCo(II)Br_2 activated with $ZnBr_2$ (purple) and Zn-reduced DPPPCo(II)Br_2 activated with NaBArF (Red) both stirred for 2 hours at the same concentrations.

Further evidence for the intermediacy of this species was from the observation of identical peak formation under two different conditions. One, upon the reduction of $(DPPP)CoBr_2$ using Zn while in the presence of NaBArF (Figure 10) or two, when isolated authentic Co(I) complex, $(DPPP)_3Co_2Br_2$ (3), was activated with NaBArF (Figure 10). A similar cationic species (5, Table 1) that is described in the literature has an absorption value at 460 nm.[19] The observed blue shift seen in this presumed metal-to-ligand charge transfer in complex 5 (5, Table 1) when compared to the $(DPPP)Co(I)^+$ species is most likely associated with the strain of the distorted tetrahedral geometry imposed by the tripodal ligand in 5.[20]

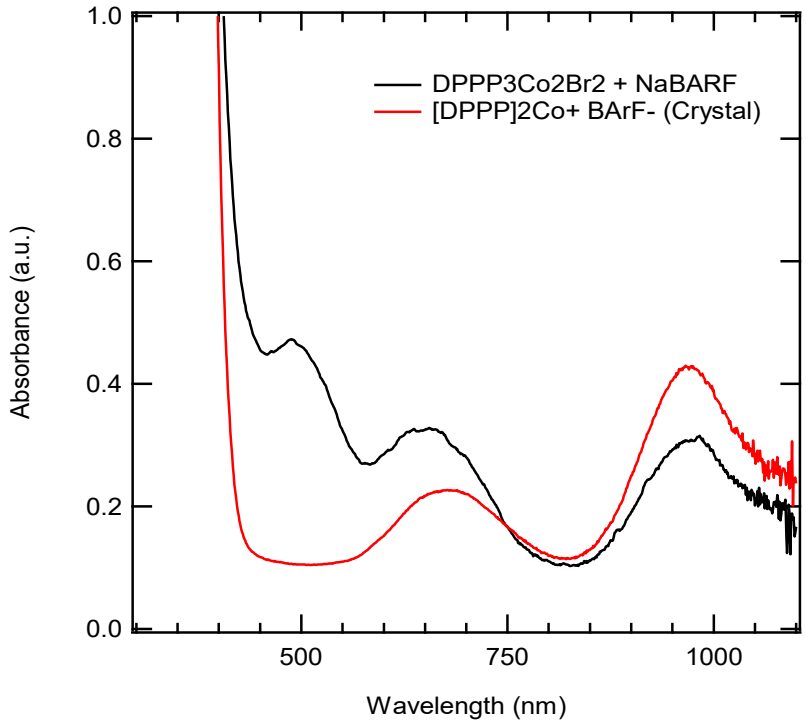

Figure 10. The UV-Vis spectrum of crystalline $(DPPP)3Co(I)Br_2$ (3), with added NaBArF (black) compared to the UV spectrum of the crystalline $[(DPPP)_2Co(I)]^+$ $BArF^-$ (7, red).

Once the activation conditions were studied via UV-Vis, efforts were made to identify, and if possible, isolate and characterize the active catalyst that is responsible for the transformation seen. Two possible situations under which the reaction could catalyze the reaction involve either

a neutral Co(I) species or a corresponding cationic $Co(I)^+$ intermediate. To verify that it was in fact the cationic species performing the reaction two parallel reactions were performed, one using (DPPP)Co(I)Br (isolated from the reduction of $(DPPP)CoBr_2$ using Zn) and the other containg DPPPCo(I)Br and $ZnBr_2$. The reaction containing DPPPCo(I)Br and no $ZnBr_2$ showed no product formation. The reaction containg both DPPPCo(I)Br and $ZnBr_2$ showed diene conversion to product, albeit in low yield. This indicates that only under conditions that favor the formation of cationic cobalt allows the reaction to proceed. This behavior has been previously observed in many other heterodimerization reactions ethylene/1,3-dodecadiene and methyl acrylate/1,3-dodecadiene dimerization reactions where several isolated neutral Co(I) complexes (e. g., (COD)η^3-cyclohepenyl), (DPPP)Co(η^3-cyclohepenyl), Zn-reduced $(DPPP)CoBr_2$ free of $ZnBr_2$) failed to effect the reaction in the absence of a Lewis acid.[9] Addition of equivalent amount of NaBArF (a bromide sequestering agent better than $ZnBr_2$) dramatically accelerates these reactions. We have seen similar behavior also in the reaction under study (2,3-dimethylbuta-1,3-diene + methyl acrylate. This strongly supports the hypothesis that the cationic cobalt is the active catalyst.

In an attempt to isolate a cationic cobalt complex that was a competent catalyst, recrystallized $Co^{(I)}$ complex $(DPPP)_3Co_2Cl_2$ (2) was further reacted with NaBARF in ether in the presence of 1,4-cyclooctadiene with the expectation to produce a substitutionally labile Co(I) complex (6, Eq 7). The reaction did not yield the expected product, but gave instead, another 16e-complex $[(DPPP)_2Co]^+$ $[BArF]^-$ (7, Eq 8), identified by X-ray crystallography (Figure 11). This complex, had a UV-Vis spectrum (675 nm, 960 nm) distinct from the species that was observed when $(DPPP)_3Co_2Cl_2$ was treated with NaBARF in that it lacked the prominent peak around 500 nm.

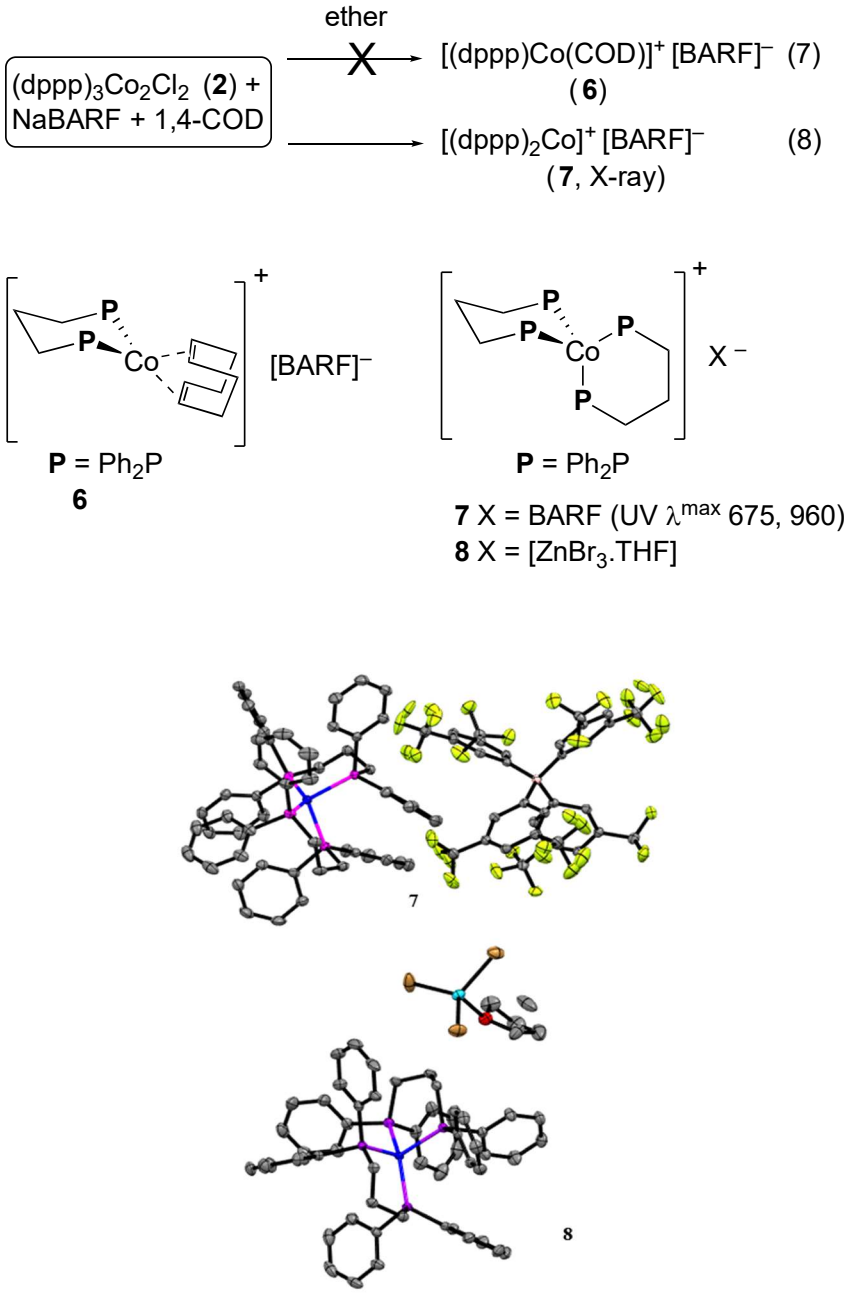

Figure 11. Solid -state structures of $[(dppp)_2Co(I)]^+$ $[BArF]^-$ (7) and $[(dppp)_2Co(I)]^+$ $[ZnBr_3.THF]^-$ (8). Hydrogens are omitted for clarity. The THF molecule in the second molecule contains a disordered carbon atom and the two positions for this disordered atom are shown in the attached ORTEP plot.

This complex did not catalyze the heterodimerization reaction under the reaction conditions. Incidentally, we had also isolated a related $[Co(I)]^+$ complex, 8, from a medium containing $(dppp)CoBr_2$, Zn and $ZnBr_2$. Collectively the above listed experiments strongly

suggested a unknown substitutionally labile cationic cobalt (I) species that was present under the reaction conditions, (DPPP)$CoBr_2$ + Zn + $ZnBr_2$ or (DPPP)$CoBr_2$ + Zn + NaBARF, was responsible for initiation of the catalytic process.

The three species of cobalt, (DPPP)Co(II)Br_2, (DPPP)Co(I)Br, and the presumed (DPPP)$Co(I)^+$ were all present under the reaction conditions (Figure 8 and 9). The generation of the presumed (DPPP)$Co(I)^+$ was shown to be cleaner under the conditions of Zn and NaBArF, as can be seen from the cleaner UV-Vis spectrum in Figure 9. Although the major peak at 517 comes from the $Co(I)^+$ species, minor peaks that are attributed to Co(II) and Co(I) can still be observed (especially under the conditions of Zn and $ZnBr_2$). This suggest that all three species are present in the start of the reaction. This further suggest that the catalyst went through two transformations prior to being able to effect the reaction that is described in Figure 9: (DPPP)Co(II)Br_2 to (DPPP)Co(I)Br, and then (DPPP)Co(I)Br to (DPPP)$Co(I)^+$, with (DPPP)$Co(I)^+$ being the active species. Therefore, If insufficient time was given to allow for these transformations, the reaction appeared initially sluggish, and the kinetic measurements were not reproducible. This behavior was exactly was observed for short stir times (<2 hours) with the induction period, but not at the longer stir times (two hours and beyond). The reproducible reaction at stir times of two hours (or greater) in conjunction with slow evolution of a catalytic species as determined by the initial UV-Vis analysis strongly supported the presence of an induction period during which the active catalytic species, $[DPPPCo^{(I)}]^+$ was produced. Thus, to obtain the highest TON and rate of reaction, the sufficient stir time of the mixture containing the pre-catalyst, reducing agent, and activator must be allowed.

2.3 Same excess experiments.

Once a both robust and reproducible experimental protocol was established for the catalytic reaction, the mechanistic investigation was continued by performing “same excess” experiments. The “same excess” experiments were used to understand the stability, the inhibition, and the deactivation of the catalyst as the reaction proceeds. For the “same excess” experiments, the difference between the molarities of the acrylate and the diene were maintained across multiple experiments, but the starting concentrations were changes (this can be seen in Table 2). The concentration profiles with respect to time for acrylate for each of the “same excess” experiments can be seen in Figure 12. As is commonly done to alleviate experimental artifacts associated with sampling, the data has been time shifted in Figure 12. This shift has occurred such that the reactions overlap at 15% conversion of the reaction conditions that had 0.36 M acrylate at 0.20 M diene (0.25 M acrylate). From the four experiments it can be seen that the decrease in concentration of acrylate with time decreases similarly regardless of the initial reaction conditions. This indicated that the number of reaction events was not affecting the catalyst and the concentration of the active catalyst was not changing as the reaction proceeded.

The overlap observed in the same excess experiments provided a key mechanistic insight. The reaction was not inhibited by the product and does not suffer appreciable catalyst deactivation in the reaction conditions. If this was the case, the same excess experiments would not overlap as they do and instead, a significant increase in rate for the lower concentration experiments would be observed. The same excess experiments also provided insight into the reason that low TON, of the magnitude of 3 to 6, were observed for this reaction. The overlap seen from the same excess experiments demonstrate that it was not the catalyst turning over to form product that was causing it to deactivate, but instead, the low TON was an issue of diene concentration in relation to the active catalyst concentration. This suggested that at low concentrations of diene, the catalyst

rapidly deactivated, limiting the TON of the reaction. This observation was critical in further work to increase the TON (*vide infra*).

Table 2. 'Same Excess' Experimental Conditions and Results

Excess Experiment	Acrylate (M)	(DPPP)$CoBr_2$ (mmol)	Zn (mmol)	$ZnBr_2$ (mmol)	Diene Conversion (%)[a]
Same Excess #1	0.26	0.152	1.52	1.58	90
Same Excess #2	0.28	0.152	1.53	1.58	91
Same Excess #3	0.31	0.152	1.52	1.57	98
Same Excess #4	0.36	0.152	1.52	1.58	89

[a] Determined by GC-FID analysis.

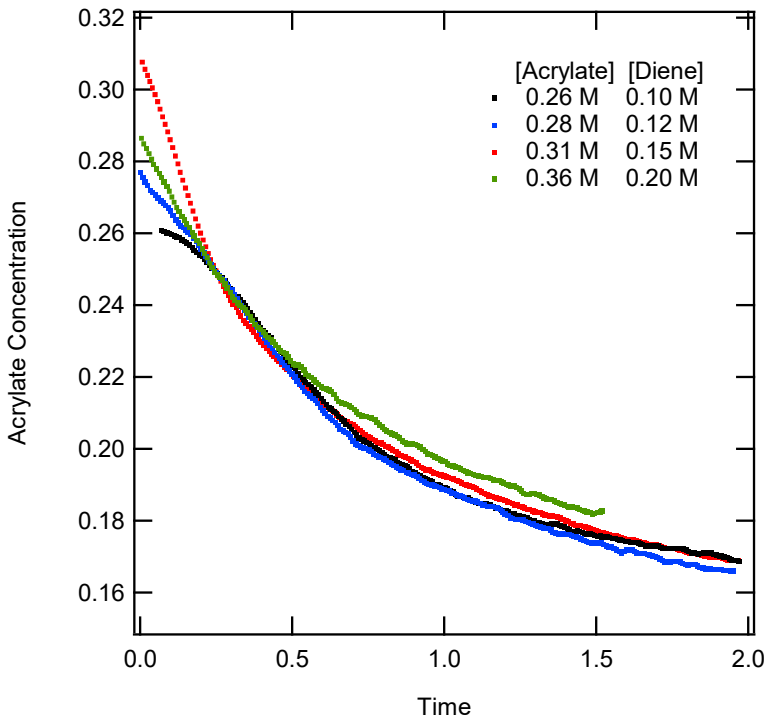

Figure 12. Acrylate concentration vs time for same excess reactions, with time shift to 15% conversion of 0.36 M acrylate and 0.10 M diene. The chart presented shows only 1 in every 10 data points collected for clarity of the figure.

2.4 Different excess experiments.

In order to investigate the order of the diene and the acrylate "different excess" experiments were performed. "Different" excess" experiment were done by varying the difference between the

molarities of the diene and acrylate. The different conditions used for these experiments can be seen in Table 3. The "different excess" experiments are best analyzed by plotting the reaction rate as a function of concentration, this can be seen in Figure 13. The standard set of conditions were 0.31 M acrylate and 0.15 diene, this reaction was performed in duplicate in order to obtain the standard deviation of the experiments and the correspondingly limitations of the analysis. Both of these experiments are shown as blue lines in figure 13.

The concentration of only the acrylate was changed across these "different excess" experiments in order to obtain the order of each of the reactants. For these reactions the diene was kept constant at 0.15 M across all three experiments while the acrylate concentration was varied from 0.17 M to 0.31 M. Both the 0.20 M and the 0.17 M acrylate different excess experiments (red and black lines respectively in Figure 13, were within the two duplicate experiments (blue lines). These results indicate that as the acrylate varies in concentration, it does not have an effect on rate of the reaction. In turn, this means that the reaction exhibits zeroth order in regards to the acrylate and does not contribute to the rate law. This statement is supported further by the data seen in Figure 13, where each of the different excess experiments were parallel and shifted to the right as the initial amount of acrylate increased. If the reaction rate was dependent on the concentration of the acrylate, one would expect the data from the different experiments to have different slopes. Both figures support the statement that acrylate was zeroth order in the reaction. Coupled with the results from the same excess experiments, it can be concluded that the reaction was first order in the diene.

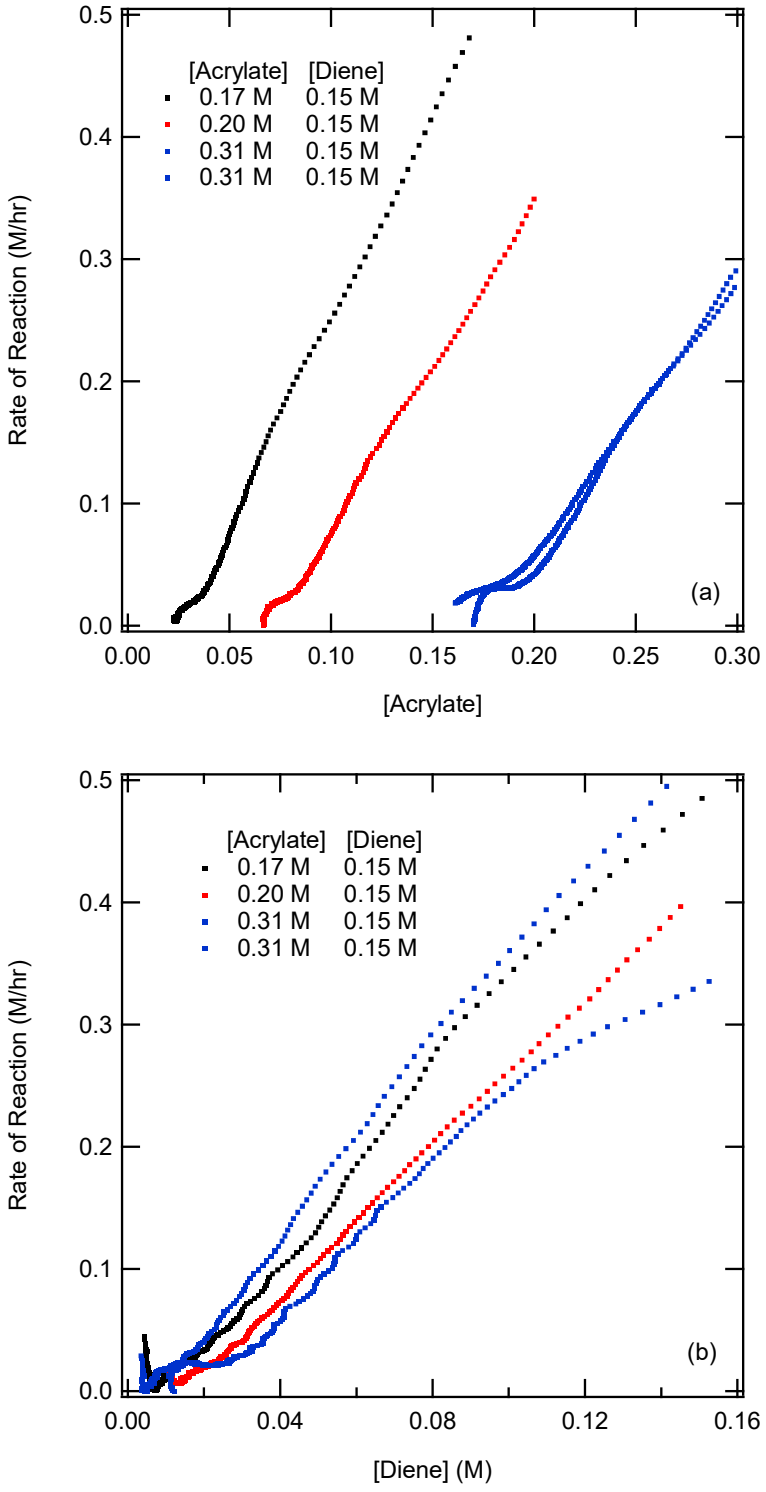

Figure 13. Different excess experiments. Diene and catalyst concentration was maintained constant at 0.152 M and 40 mM respectively where the acrylate concentration was varied 0.17 M (black), 0.20 M (red) and 0.31 M (blue). (a) Diene rate vs diene concentration for different excess experiments. (b) Acrylate rate vs acrylate concentration for different excess test.

Table 3. Different Excess Experimental and Conditions

'Different Excess' Experiment	Acrylate (M)	(DPPP)$CoBr_2$ (mmol)	Zn (mmol)	$ZnBr_2$ (mmol)	Conversion of diene (%)[a]
Different Excess #1	0.17	0.152	1.52	1.58	97
Different Excess #2	0.20	0.153	1.53	1.58	92
Different Excess #3	0.31	0.151	1.55	1.57	94
Different Excess #4	0.31	0.152	1.52	1.57	98

[a] Determined by GC-FID analysis.

2.5 Order in the catalyst.

An important component to the overall catalytic cyce was the order of the catalyst. The effects that different catalyst loading ahd on the reaction order was investigated using a range of 0.20 mM to 0.40 mM catalyst. The values for the diene and acrylate concentration in the model were kept constant at 0.15 M and 0.31 M respectively. For the model the catalyst concentration was set to 0.20 mM, 0.30 mM, and 0.40 mM. From the experimental data, the reaction rate was determined as a function of diene concentration. As would be expected the rate decreases when less catalyst was used. The experimental data for 0.20 mM catalyst was used to determine an experimental reaction rate constant (k). The rate constant was found to be 79.6 min^{-1}. Using this rate constant, a model fit assuming that the catalyst was 1st order was calculated, as shown in Figure 14. Excellent agreement is observed between the experimental values and the model for the 0.20 mM, 0.30 mM, and 0.40 mM catalyst trials. The results were consistent with the reaction being first order in the catalyst. Therefore, the experimental data indicated that the amount of active catalyst was proportional to the amount of active Co(I) present.

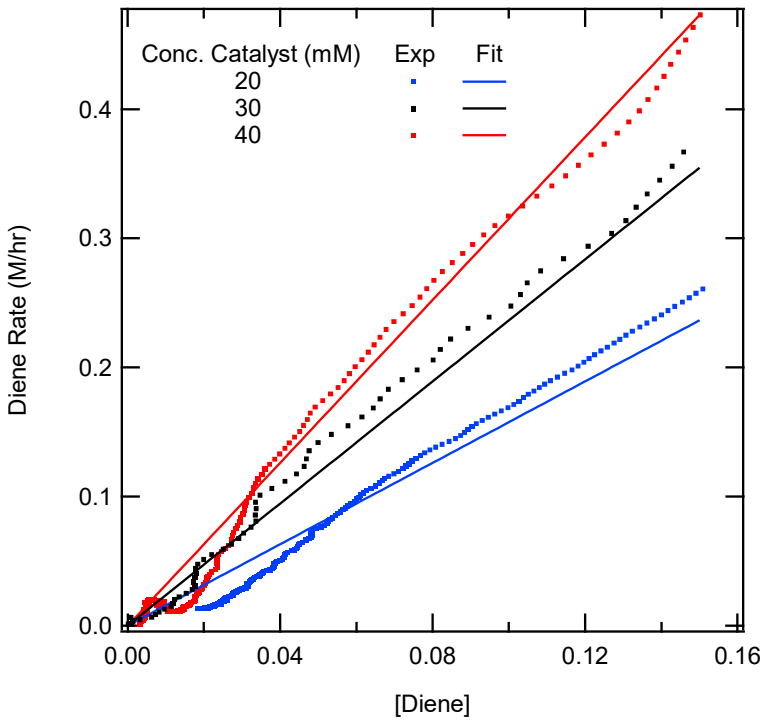

Figure 14. Rate of diene conversion vs diene concentration with first order catalyst model overlaid. The model was prepared by graphing first order rates using the rate law: rate = k[diene][cat], where the diene concentration and catalyst loading were used as appropriate. The conditions for each experiment are: 20 mM catalyst, 0.31 M acrylate, and 0.15 M diene (blue), 30 mM catalyst, 0.31 M acrylate, and 0.15 M diene (black), 40 mM catalyst, 0.31 M acrylate, and 0.15 M diene (red).

2.6 Catalyst deactivation.

The stability of the reduced catalyst precursor (in the absence of substrates, coordinating solvent or excess reducing agent) was examined by monitoring the peak at 517 nm, Figure 15. The peak at 517 nm was formed under reaction conditions, as shown in Figure 15 and appears only after treatment of the Co(I) bromide with a Lewis acid, causing the peak to be attributed to the $[(DPPP)Co^{(I)}]^{+}$ species. Even under conditions that was free of both moisture and oxygen, the peak at 517 nm still decreased as time progressed, this can be seen in Figure 15. At first, this statement seems counterintuitive to the conclusions drawn about the induction period and drawn from the same excess experiments, however, it can be explained. Under the reaction conditions seen in the "same excess" and stir time experiments there was a large amount of excess Zn and $ZnBr_2$. Both

of these species were responsible for the formation of the active $[DPPPCo^{(I)}]^+$. Since Zn and $ZnBr_2$ were present in large excess, any catalyst that deactivated (possibly by redox processes/ disproportionation) could be immediately activated again. This was not the case for the results seen in Figure 6, where only the supernatant was analyzed via UV-Vis, after filtering off the insoluble Zn and $ZnBr_2$. In these tests, only the catalyst itself existed in solution, meaning it could not be re-activated. Therefore, the decay of the 517 nm peak was considered characteristic of an unstable species.

While the cationic cobalt was unstable in pure solvent, it was possible that the catalyst could be stabilized by the presence of the diene and/or the acrylate. The stability of the catalyst in the presence of the different was evaluated, this can be seen in Figure 15. Addition of acrylate to the active catalyst showed an immediate decrease in the intensity of the peaks that correspond to the $Co(I)^+$ species (517 nm) and an increase of the peaks that correspond to the Co(II) species (660 and 735 nm). Note the peak at 660 nm seemed unchanged, but recall the solution was being diluted during addition of a solution of the acrylate. This strongly suggest that the acrylate is unable to stabilize the active catalyst to any measurable means. Diene addition (Figure 15) to the active catalyst showed a decrease in the peak that corresponds to the active catalyst (517 nm), however, this decrease was appreciably slower than that of the acrylate addition. More importantly, the addition of diene caused peaks that correspond to the Co(II) species to decrease in intensity. This suggested that the diene was able to stabilize the active low-valent catalytic species and prevent degradative pathways that led to the formation of potentially nonactive Co(II) species.

Further support for the diene being able to stabilize the active catalytic species was observed upon adding both diene and acrylate to the active catalyst, Figure 15. The acrylate was added to the active catalyst first and after five minutes, the diene was added to the cuvette.

Addition of the acrylate showed the behavior described above. However, upon addition of the diene, the UV-Vis spectrum changed according to the above description following the diene addition. This suggested that diene was able to bind more strongly to the active catalyst than the acrylate, and in turn, prevent the degradation of the active catalyst to nonactive Co(II) species. From the UV-Vis experiments, it was found that the reduced catalyst precursor was an unstable species and needed a coordinating agent around to limit catalyst deactivation. Diene was such a species, that the diene would bind more strongly to the active catalyst than acrylate in that process affording more stabilization than the acrylate.

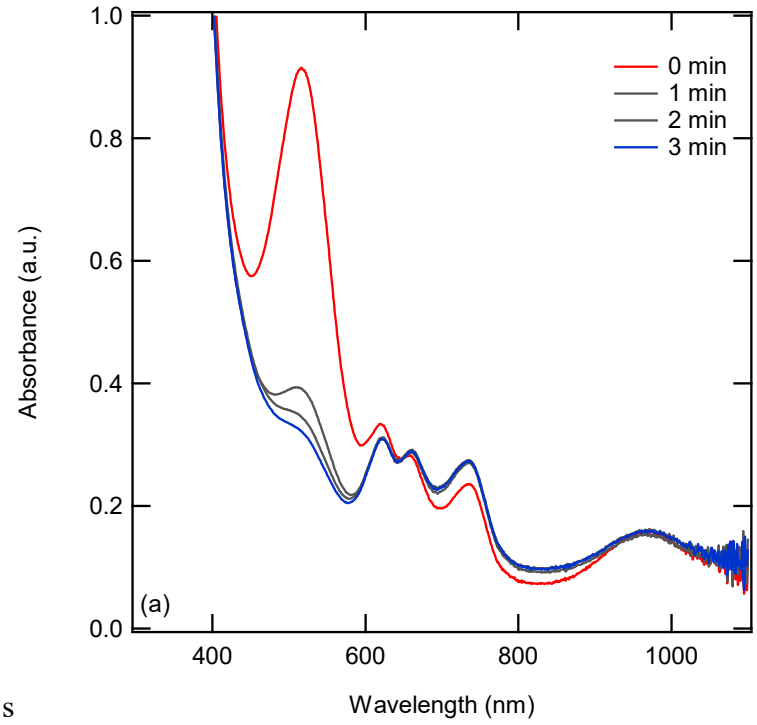

s

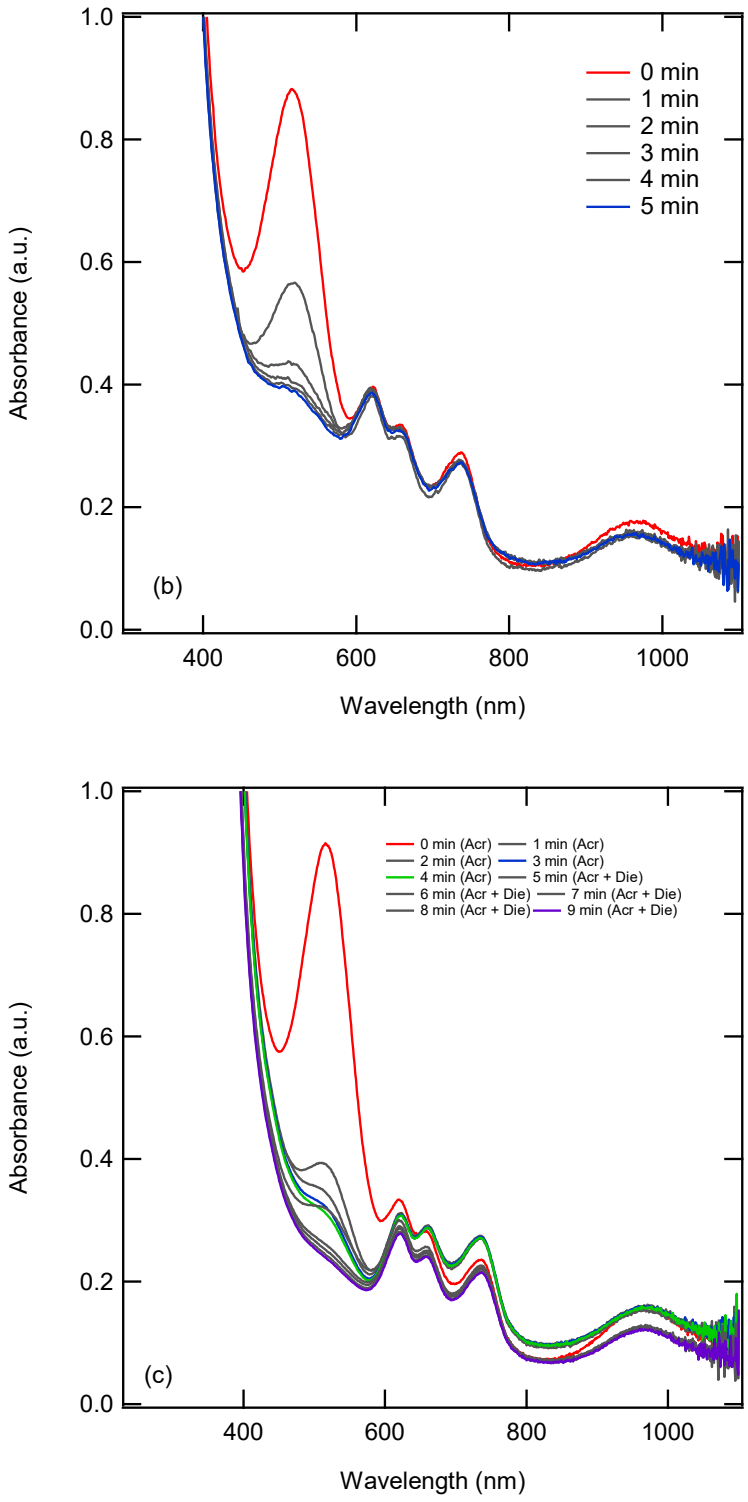

Figure 15. (a) The supernatant of a reaction mixture of (DPPP)Co(II)Br_2, Zn, and $ZnBr_2$ was stirred for two hours after which, the following was carried out: Methyl acrylate in DCE (0.11 mmoles, 0.22 M, 58 eq with respect to cobalt species) added to $[(DPPP)Co(I)]^+$ (0.0038 mmole, 1.9 mM). Spectra were taken for 3 min with 1 min interval. (c) The supernatant of a reaction mixture of (DPPP)$Co^{(II)}Br_2$, Zn, and $ZnBr_2$ was stirred for two hours after which, the following was added:. 2,3-dimethyl-1,3-

butadiene in DCE added (0.044 mmoles, 0.044 M, 11.63 eq with respect to cobalt species) added to $[DPPPCo^{(I)}]^+$ (0.0038 mmole, 19 mM). Spectra taken for 5 min with 1 min interval. (C) The supernatant of a reaction mixture of $(DPPP)Co^{(II)}Br_2$, Zn, and $ZnBr_2$ was stirred for two hours after which, the following was carried out: methyl acrylate in DCE (0.11 mmoles, 0.22 M, 58 eq with respect to cobalt species) was added to $[(DPPP)Co(I)]^+$ (0.0038 mmole, 1.9 mM). Readings were taken for 4 minutes. Then 2,3-dimethyl-1,3-butadiene in DCE added (0.044 mmoles, 0.044 M, 11.63 eq with respect to cobalt species) was added to $[(DPPP)Co(I)]^+$ (0.0038 mmole, 19 mM), readings were taken for another 5 minutes.

2.7 Reversibility and summary of catalytic cycle and rate law.

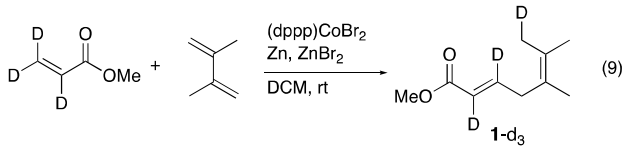

Figure 16. Deuterium labeling experiment performed to test for reversibility.

The reversibility of the reductive elimination step Figure 2 (the catalytic cycle A/B) was investigated via a deuterium labeling experiment (Eq 9). The product of the above reaction (methyl acrylate d_3 reacted with 2,3-dimethyl-1,3-butadiene) was characterized by both ^{13}C and ^{1}H NMR. Using an inverse gated decoupling experiment ($^{13}C\{^{1}H\}$) the ^{13}C NMR was used to obtain quantitative information on the incorporation of deuterium. The deuterium attachment to the methyl group in product-d_3 shifted the corresponding ^{13}C NMR peak by approximately 0.3 δ and caused a triplet to form (20.24 ppm to 19.96 ppm).[22] Using this information, it was found that the CH_2D peak, when compared to the intensity of its neighboring CH_3 peak, integrated as 0.96 to 1.00, suggesting a 96% deuterium incorporation. This strongly suggested that the β-hydride elimination step in the proposed mechanistic cycles were not reversible.

A mechanism that was consistent with all the available experimental observations was the oxidative dimerization route, shown in Figure 2 **B**. More intimate details of this mechanism were shown in Figure 17. The UV-Vis competition experiments suggested that the diene coordinated to the active catalyst (**A**) much more quickly than the acrylate. It was hypothesized that after the coordination to form **B**,[19, 23] the diene undergoes oxidative cyclization giving a metallacyclic species (**C**) in which cobalt was in the +3 oxidation state. This change was consistent with the

rapid disappearance of the UV absorption at 517 nm. It was postulated that cobaltacycle forms, followed by the acrylate quickly coordinating to the intermediate to give **D**. Subsequently a migratory insertion took place to give yet another metallacycle **E**. A β-hydride elimination occurred to give **F**. Reductive elimination returned the Co to oxidation state (III), giving the complex **G**. The turn over limiting step was most likely the displacement of the product **1** by 2,3-methyl-1,3-butadiene to regenerate **B**, which in subsequent oxidative cyclization gave **C**. From the UV-Vis studies, it was found that the initial coordination of either acrylate or diene to the [Co $^{(I)}]^+$ species was very facile, in both the individual and the competition study, less than 1 minute. Thus, coordination of the diene to the (DPPP)Co(I)$^+$ as envisioned in the first step **A** → B cannot be the turnover limiting step. By contrast, generation of **B** from **G** could be slower. Thus, **G** could be thought of as the catalyst resting state.

2.8 Reaction engineering.

From the above kinetic and mechanistic investigation three major findings were made. One, the active catalyst was uninhibited by either diene or acrylate. Furthermore, the catalyst deactivation was not attributed to how many turnovers it performed, but instead, stability of the putative Co(I)$^+$ intermediate at low concentrations of a stabilizing substrate. The reaction was first order in diene and the catalyst, with only diene being represented in the rate law of the reaction. This signified that to increase the rate of the reaction the concentration of diene needed to be increased and, this could be done without any deleterious effect on the reaction since, as already stated, neither diene nor acrylate, inhibited the reaction. Three, compared to acrylate, diene was a stronger chelator to the active catalyst, (DPPP)Co(I)$^+$.

With this information in mind, the reaction parameters were changed in an effort to increase the TON. A high concentration of diene and acrylate were used in a batch reaction since a high

concentration was likely to both stabilize the catalyst while at the same time increase the rate of the reaction. Thus, instead of a 0.15 M diene and a 0.31 M acrylate, a 3.0 M diene and 3.2 M acrylate reaction was performed under otherwise similar concentration of the catalyst. Under these conditions, the product was formed with a yield of 48% in 18 h, improving the TON by nearly a factor of 10. Clearly, understanding the mechanism of the reaction helped to improve the overall efficiency of the reaction. These studies suggested that the cationic Co(I) catalyst was inherently prone to deactivation by hither to unknown mechanisms, including possible formation of a tetraligated Co(I) species **I** (Figure 11) that *does not catalyze* the reaction. Improvements in the design of ligands might alleviate this situation. One intriguing possibility would be to use a bidentate ligand with an additional possibility of an internal hemilabile coordination to stabilize any putative coordinately unsaturated cobalt intermediates. Previously, this strategy had been found to be useful in the discovery of highly efficient nickel catalysts (TON >7000) for asymmetric hydrovinylation of vinylarenes.[24] In that instance, a highly unstable coordinately unsaturated Ni(II) intermediate was stabilized by a hemilabile pendant group.

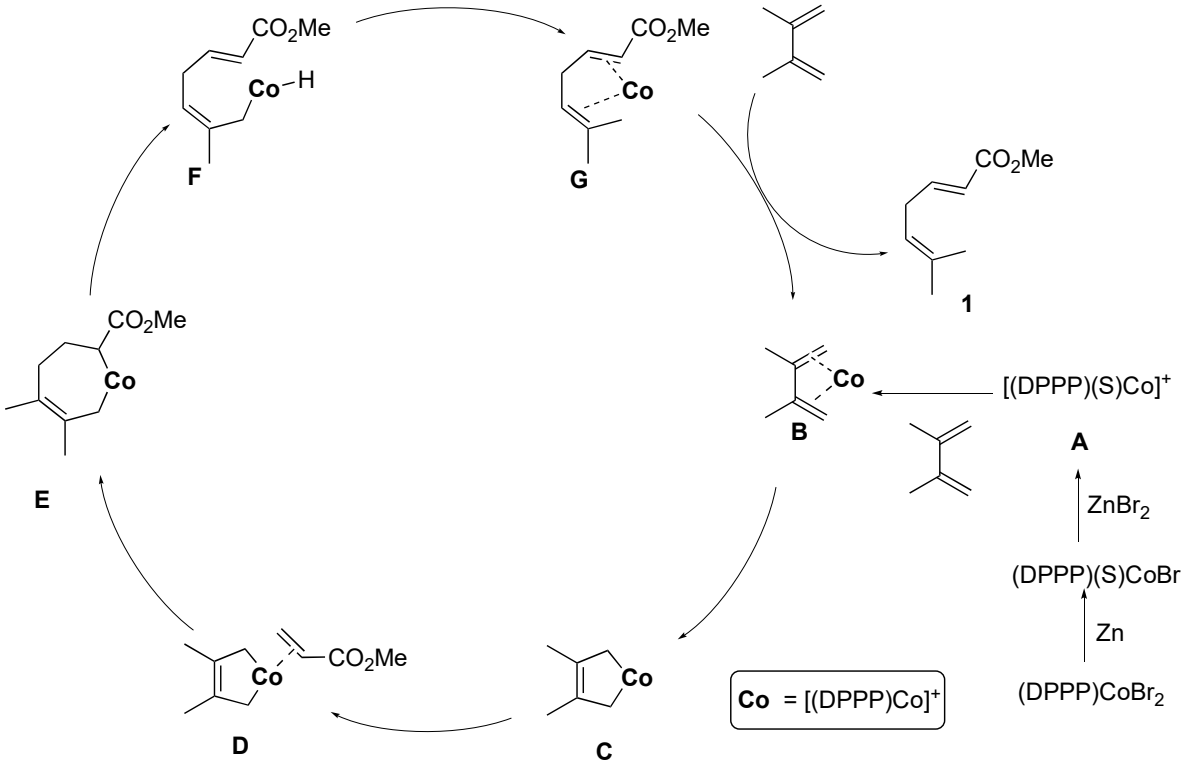

Figure 17. A proposed mechanism consistent with experimental observations.

2.9 Conclusions.

1,3-Dienes and alkyl acrylates, two of the most abundant feedstock starting materials, undergo highly selective co-dimerization in the presence of Zn-reduced (*bis*-phosphine)CoX_2 complexes and a halide sequestering agent such as $ZnBr_2$. Recent advances in synthetic methodology have allowed highly enantioselective coupling (enantiomeric ratios >95:5) of these relevant partners; yet, the efficiency as measured by the TON in the catalyst for these reactions remained modest. For any large-scale applications, more efficient processes have to be developed. Understanding the mechanism of the reaction is the first step in this process towards increasing the catalytic efficiency. Through isolation and characterization of possible low-valent cobalt precursors involved and a study of the reaction profile using reaction progress kinetic analysis (RPKA), several important details of the mechanism have emerged. For example, it was found

that the reaction had an induction period that required at least two hours of stir time to generate the competent catalyst. Further investigation of the induction period using UV-Vis analysis revealed that transformation of Co(II) to Co(I), and subsequently to a cationic $[Co(I)]^+$ species was responsible for this delay for the onset of the reaction. Through RPKA using in situ IR spectroscopy, same excess experiments demonstrated that the catalyst was not inhibited by the starting materials or the products, and the low TON observed was a result of the inherent instability of the putative cationic Co(I)-species that catalyzes the reaction. Different excess experiments provided insights that the rate law for the reaction that was first order in the diene and zeroth order in the acrylate. Catalyst loading experiments showed that the catalyst was first order. Variable time normalization methods were also performed and confirmed the order of the catalyst and reagents.[25] From this detailed understanding of the reaction, a mechanism was proposed and based on the conclusions of this study it was possible to increase the TON by a factor of 10 by conducting the reaction at an increased concentration of the starting materials, especially, the diene, which seemed to stabilize the catalytic species. Isolation and identification of a catalytically inactive tetra-ligated cationic Co(I) complex suggested that the formation of such a species may be one mode of deactivation of the catalyst.

2.10 References

1. (a)Cornils, B.; Herrmann, W. A. *Applied Homogeneous Catalysis with Organometallic Compounds*; VCH: New York, 1996; Vol. 1 and 2; (b) Schaub, T.; Hashmi, A. S. K.; Paciello, R. A. Tackling Challenges in Industrially Relevant Homogeneous Catalysis: The Catalysis Research Laboratory (CaRLa), an Industrial–Academic Partnership. *J. Org. Chem.* **2018**, *84,* 4604-4614 (c) Shi, S. L.; Wong, Z. L.; Buchwald, S. L. Copper-catalysed

enantioselective stereodivergent synthesis of amino alcohols. *Nature* **2016**, *532*, 353-356; (d) Liao, K.; Negretti, S.; Musaev, D. G.; Bacsa, J.; Davies, H. M. L. Site-selective and stereoselective functionalization of unactivated C-H bonds. *Nature* **2016**, *533*, 230-234; (e) Zhang, W.; Wang, F.; McCann, S. D.; Wang, D. H.; Chen, P. H.; Stahl, S. S.; Liu, G. S. Enantioselective cyanation of benzylic C-H bonds via copper-catalyzed radical relay. *Science* **2016**, *353*, 1014-1018; (f) Mlynarski, S. N.; Schuster, C. H.; Morken, J. P. Asymmetric synthesis from terminal alkenes by cascades of diboration and cross-coupling. *Nature* **2014**, *505*, 386-390; (g) Zbieg, J. R.; Yamaguchi, E.; McInturff, E. L.; Krische, M. J. Enantioselective C-H crotylation of primary alcohols via hydrohydroxyalkylation of butadiene. *Science* **2012**, *336*, 324-327; (h) Zuend, S. J.; Coughlin, M. P.; Lalonde, M. P.; Jacobsen, E. N. Scaleable catalytic asymmetric Strecker syntheses of unnatural-amino acids. *Nature* **2009**, *461*, 968-970. (i) Schaus, S. E.; Brandes, B. D.; Larrow, J. F.; Tokunaga, M.; Hansen, K. B.; Gould, A. E.; Furrow, M. E.; Jacobsen, E. N. Highly selective hydrolytic kinetic resolution of terminal epoxides catalyzed by chiral (salen)CoIII complexes. Practical synthesis of enantioenriched terminal epoxides and 1,2-diols. *J. Am. Chem. Soc.* **2002**, *124*, 1307-1315.

2. (a) Hirano, M. Recent advances in the catalytic linear cross-dimerizations. *ACS Catalysis* **2019**, *9*, 1408-1430; (b) Chauvin, Y.; Olivier, H. Dimerization and Codimerization In *Applied Homogeneous Catalysis with Organometallic Compounds*; Cornils, B., Herrmann, W. A., Eds.; VCH: New York, 1996; Vol. 1, pp. 258-268. (c) RajanBabu, T. V.; Cox, G. A.; Lim, H. J.; Nomura, N.; Sharma, R. K.; Smith, C. R.; Zhang, A. Hydrovinylation Reactions in Organic Synthesis in *Comprehensive Organic Synthesis, 2nd Edition*; Molander, G. A., Knochel, P., Eds.; Elsevier: Oxford, 2014; Vol. 5, pp 1582-1620. (d) Hilt, G.; Luers, S.

Cobalt(I)-catalyzed 1,4-hydrovinylation reactions of 1,3-dienes with functionalized terminal alkenes under mild conditions. *Synthesis* **2002**, 609-618. (e) Lo, J. C.; Kim, D.; Pan, C.-M.; Edwards, J. T.; Yabe, Y.; Gui, J.; Qin, T.; Gutiérrez, S.; Giacoboni, J.; Smith, M. W.; Holland, P. L.; Baran, P. S. Fe-Catalyzed C–C bond construction from olefins via radicals. *J. Am. Chem. Soc.* **2017**, *139*, 2484-2503.

3. (a) Koltzenburg, S.; Maskos, M.; Nuyken, O. *Polymer Chemistry*; Springer-Verlag: Berlin, 2017. (b) Dimersol technology (propylene dimerization): Bogdanovi´c, B.; Henc, B.; Löser, A.; Meister, B.; Pauling, H.; Wilke, G. Use of cationic nickel for olefin dimerization. *Angew. Chem. Int. Ed. Engl.* **1973**, *12*, 954-964. (c) Shell Higher Olefin Process via ethylene oligomerization: Keim, W. Oligomerization of ethylene to α-olefins: Discovery and development of the Shell higher olefin process (SHOP). *Angew. Chem., Int. Ed.* **2013**, *52*, 12492−12496. (e) Speiser, F.; Braunstein, P.; Saussine, L. Catalytic ethylene dimerization: Recent developments with nickel complexes containing *P,N*-chelating ligands. *Acc. Chem. Res.* **2005**, *38*, 784-793.
4. Su, A. C. L. Codimerization of ethylene and butadiene. *Adv. Organomet. Chem.* **1979**, *17*, 269-318.
5. Wittenberg, D. Novel dienylation reactions. *Angew. Chem. Int. Ed.* **1964**, *3*, 153.
6. (a) Feldman, K. S.; Grega, K. C. Cobalt mediated alkene diene coupling - documentation of scope, limitations, and regioselectivity. *J. Organomet. Chem.* **1990**, *381*, 251-260; (b) Mitsudo, T.-a.; Zhang, S. W.; Kondo, T.; Watanabe, Y. Ruthenium complex-catalyzed selective syntheses of 3,5-dienoic acid derivatives by coupling of 1,3-dienes or allylic carbonates with acrylic compound. *Tetrahedron Lett.* **1992**, *33*, 341-344.

7. (a) Hilt, G.; du Mesnil, F. X.; Luers, S. An efficient cobalt(I) catalyst system for the selective 1,4-hydrovinylation of 1,3-dienes. *Angew. Chem. Int. Ed.* **2001**, *40*, 387-389; (b) Erver, F.; Hilt, G. Multi-component regio- and diastereoselective cobalt-catalyzed hydrovinylation/allylboration reaction sequence. *Org. Lett.* **2011**, *13*, 5700-5703.
8. (a) Hiroi, Y.; Komine, N.; Komiya, S.; Hirano, M. Regio- and enantioselective linear cross-dimerizations between conjugated dienes and acrylates catalyzed by new Ru(0) complexes. *Organometallics* **2014**, *33*, 6604-6613; (b) Hirano, M.; Tanaka, Y.; Komine, N. Synthesis of and catalytic linear cross-dimerizations by an electron-deficient cyclic diene complex of ruthenium(0). *Organometallics* **2018**, *37*, 4173-4176.
9. Jing, S. M.; Balasanthiran, V.; Pagar, V.; Gallucci, J. C.; RajanBabu, T. V. Catalytic enantioselective hetero-dimerization of acrylates and 1,3-dienes. *J. Am. Chem. Soc.* **2017**, *139*, 18034-18043.
10. See chapter 3 for information regarding general procedures.
11. Joseph, J.; RajanBabu, T. V.; Jemmis, E. D. A Theoretical investigation of the Ni(II)-catalyzed hydrovinylation of styrene. *Organometallics* **2009**, *28*, 3552-3566.
12. (a) Hilt, G.; Treutwein, J. Cobalt-catalysed hydrovinylation as the key step in a short synthesis of moenocinol. *Chem. Commun.* **2009**, 1395-1397. (b) Timsina, Y. N.; Sharma, R. K.; RajanBabu, T. V. Cobalt-catalyzed asymmetric hydrovinylation of 1,3-dienes. *Chem. Sci.* **2015**, *6*, 3994-4008.
13. (a) Hirano, M.; Ueda, T.; Komine, N.; Komiya, S.; Nakamura, S.; Deguchi, H.; Kawauchi, S. Mechanistic insights into catalytic linear cross-dimerization between conjugated dienes and styrenes by a ruthenium(0) comple. *J. Organomet. Chem.* **2015**, *797*, 174-184; (b) Hirano, M.; Komiya, S. Oxidative coupling reactions at ruthenium(0) and their applications

to catalytic homo- and cross-dimerizations. *Coord. Chem. Rev.* **2016**, *314*, 182-200. (c) For an oustanding investigation of the mechanism of Fe-catalyzed heterodimerization of 1,3-dienes and *n*-alkenes, see: Schmidt, V. A.; Kennedy, C. R.; Bezdek, M. J.; Chirik, P. J. Selective [1,4]-hydrovinylation of 1,3-dienes with unactivated olefins enabled by iron diimine catalysts. *J. Am. Chem. Soc.* **2018**, *140*, 3443-3453. (d) See also ref 2(e) for mechanistic studies of an Fe-catalyzed olefin cross-coupling reactions.

14. (a) Blackmond, D. G. Reaction progress kinetic analysis: A powerful methodology for mechanistic studies of complex catalytic reactions. *Angew. Chem. Int. Ed.* **2005**, *44*, 4302-4320. (b) Blackmond, D. G. Kinetic profiling of catalytic organic reactions as a mechanistic tool. *J. Am. Chem. Soc.* **2015**, *137*, 10852-10866.
15. (a) Analysis of the IR spectrum of methyl acrylate: Carmona, P.; Moreno, J. The infrared spectra and structure of methyl acrylate. *J. Mol. Struct.* **1982**, *82*, 177-185. (b) Analysis of the IR spectrum of 2,3-dimethylbutadiene: Durig, J. R.; Compton, D. A. C. Analysis of torsional spectra of molecules with two internal C3v rotors. 16. Infrared and Raman spectra, vibrational assignment, methyl torsional potential function, and gas phase thermodynamic functions of 2,3-dimethylbuta-1,3-diene. *J. Phys. Chem.* **1979**, *83*, 2879-2886.
16. Quotation marks were placed around the formula for these species since the exact identity of this coordinately unsaturated complex is not known, and it may involve coordination to a reagent or solvent, or intermolecular bridging through DPPP ligands (See text).
17. (a) Aresta, M.; Rossi, M.; Sacco, A. Tetrahedral complexes of cobalt(I). *Inorg. Chim. Acta* **1969**, *3*, 227-231 (b) Krzystek, J.; Ozarowski, A.; Zvyagin, S. A.; Telser, J. High spin Co(I): High-frequency and -field EPR spectroscopy of $CoX(PPh_3)_3$ (X = Cl, Br). *Inorg. Chem.*

2012, *51*, 4954-4964. (c) Heinze, K.; Huttner, G.; Zsolnai, L.; Schober, P. Complexes of cobalt(II) chloride with the tripodal trisphosphane triphos: Solution dynamics, spin-crossover, reactivity, and redox activity. *Inorg. Chem.* **1997**, *36*, 5457-5469.

18. Preparation and characterization including solid-state structures of $[(dppp)_3Co_2Cl_2]$ (**2**), CCDC accession number 1873380 and $[(dppp)_3Co_2Br_2]$ (**3**), CCDC accession number 1814337 have been reported. See ref 21(a) and ref 9) respectively.
19. (19) Rupp, R.; Frick, A.; Huttner, G.; Rutsch, P.; Winterhalter, U.; Barth, A.; Kircher, P.; Zsolnai, L. eta-(4)-coordination of dienes and heterodienes to the tripod-cobalt(I) template $[CH_3C(CH_2PPh_2)_3(Co)]^+$: Synthesis, structure, and dynamics. *Eur. J. Inorg. Chem.* **2000**, 523-536.
20. Rose, M. J.; Bellone, D. E.; Di Bilio, A. J.; Gray, H. B. Spectroscopic and magnetic properties of an iodo Co-I tripodal phosphine complex. *Dalton Transactions* **2012**, *41*, 11788-11797.
21. Use of NaBARF gives the best reactions in cross-dimerizations, hydroboration and [2+2]-cycloadditions. (a) Duvvuri, K.; Dewese, K. R.; Parsutkar, M. M.; Jing, S. M.; Mehta, M. M.; Gallucci, J. C.; RajanBabu, T. V. Cationic Co(I)-intermediates for hydrofunctionalization reactions: regio- and enantioselective cobalt-catalyzed 1,2-hydroboration of 1,3-dienes. *J. Am. Chem. Soc.* **2019**, *141*, 7365-7375. (b) Parsutkar, M. M.; Pagar, V. V.; RajanBabu, T. V. Catalytic enantioselective synthesis of cyclobutenes from alkynes and alkenyl derivatives. *J. Am. Chem. Soc.* **2019**, *141*, xxxxx-xxxxx. DOI: 10.1021/jacs.9b07885.
22. MacDougal J., Simpson M., Cole-Hamilton D.: Comparison of carbon-13 nuclear magnetic resonance methods for the analysis of multiple partially deuterated products from

catalytic reactions: heptan-1-ol and 2-methylpropanol. *J. Chem. Soc. Dalton Trans.* **1994**, 20,3061-3065.

23. For a related cationic complex of Co(I), see ref. 19.

24. (a) Nandi M., Jin J., and, and RajanBabu T.V. Synergistic effects of hemilabile coordination and counterions in homogeneous catalysis: New tunable monophosphine ligands for hydrovinylation reactions. *J. Am. Chem. Soc.* **1999,** 121*,* 9899-9900. (b) Smith, C. R.; RajanBabu, T. V. Efficient, selective, and green: catalyst tuning for highly enantioselective reactions of ethylene. *Org. Lett.* **2008**, *10*, 1657-1659.

25. (a) Nielsen C., Bures J. Visual Kinetic Analysis. *Chem. Sci.,* **2019**, 10, 348. (b) Bures J. A simple Graphical Method to Determine the Order in Catalyst. *Angew. Chem. Int. Ed.* **2016**, 55, 2028-2031. (c) unpublished results by Gray et al. (full details will appear in the publication currently under review).

Chapter 3: Experimental Information

3.1 General Methods

All use of moisture and oxygen sensitive materials were handled using standard Schlenk techniques under an argon atmosphere or in a glove-box under a nitrogen atmosphere maintained at less than 5 ppm oxygen. The Schlenk line was attached to a vacuum pump that was kept between 0.2 and 0.01 mm Hg for all evacuations and drying of air sensitive compounds. Before use, all glassware is washed by soaking it in an base bath (isopropanol and KOH) overnight (12 h), rinsing with water, then soaking in an acid bath overnight (12 h), then rinsed a second time with water and dried with acetone. The glassware was stored in an oven for 12 h that was set at 160 ºC.

All gas chromatographic analysis of the reactions were performed on an Agilent 6850 G.C. with a HP-1 methyl siloxane column (30 m, 0.32 mm ID, 0.25 μm) and hydrogen carrier gas with FID-detector at 250 ºC. The method of analysis: initial temperature 50 ºC held for 5 min, ramp 10 ºC/min to 70 ºC, held for 15 min ramp 20 ºC/min to 250 ºC held for 5 min.

Proton and carbon nuclear magnetic resonance spectra (^{1}H and ^{13}C) were recorded on a Bruker Avance III HD Ascend 400 MHz SPX equipped with an inverse probe and for deuterium labeling experiments a Bruker Avance III HD Ascend 600 MHz SPX was used. Solvent resonance was used as an internal standard for the chemical shifts, $CDCl_3$ at 7.26 ppm for ^{1}H NMR and $CDCl_3$ at 77.16 ppm for ^{13}C NMR. NMR data are reported as the following: Chemical shift, multiplicity (s = singlet, d = doublet, t = triplet, q = quartet, pent = pentet, m = multiplet, dd = doublet of doublet, dt = doublet of triplet), coupling constants (Hz), and integration.

All UV-Vis spectra were collected on an Agilent Cary 60 spectrophotometer outfitted with stirring capabilities at room temperature (22 ^{o}C). All IR spectra were collected on a Mettler Toledo ReactIR 45m instrument.

3.2 Chemicals

The chemicals used for the experiments were as follows: Diethyl ether (Fischer Scientific, Anhydrous), tetrahydrofuran (Alfa Aesar, 99%), hexanes (Sigma Aldrich, ≥ 98.5%), pentanes (Sigma Aldrich, ≥ 99%), 1,2-dichloroethane (Sigma Aldrich, ≥ 99%), dichloromethane (Sigma Aldrich, ≥ 99.8%, 40-150 ppm amylene), methyl acrylate (Sigma Aldrich, 99%, ≤ 100 ppm monomethyl ether hydroquinone), 2,3-dimethyl-1,3-butadiene (Alfa Aesar, 98%, 100 ppm BHT), Zinc (Sigma Aldrich), $CoBr_2$ (Sigma Aldrich, 99%), $ZnBr_2$ (Sigma Aldrich, 98%, Anhydrous), and 1,3-Bis(diphenylphosphino)propane (Sigma Aldrich, 97%).

3.3 Purification methods

3.3.1 Purification of solvents and storage of purified chemicals

Diethyl ether, tetrahydrofuran, hexanes, and pentanes were freshly distilled prior to each reaction. They were distilled over Na metal and allowed to cool to room temperature before use. 1,2-Dichloroethane and dichloromethane were freshly distilled prior to each reaction. The solvents were distilled over CaH_2 and allowed to cool to room temperature before their use in reactions.

3.3.2 Distillation of methyl acrylate[1]

Methyl acrylate, (50.00 mL, 47.80 g, 0.555 moles), was added to a 100 mL beaker. The methyl acrylate was washed with 2 M NaOH (20 mL portions, 3 times) and then washed with distilled water (20 mL portions, 3 times) in order to get wash the methyl acrylate clean of the inhibitor monomethyl ether hydroquinone. The washed methyl acrylate is added to a 100 mL round bottom flask equipped with a magnetic stirrer and $CaCl_2$ (0.50 g, 0.0045 moles). A short-path distillation apparatus is attached to the round bottom flask, and the apparatus is added to an oil bath at 60 ºC. The fractional distillation is then carried out under reduced pressure (via a Schlenk line 0.2 to 0.01 mmHg). After distillation, the acrylate is partitioned into two 20 mL oven dried glass vials. The vials are then wrapped in black electrical tape and stored in a freezer, while not in use, set to -4 ºC. Before use, the methyl acrylate is taken out and allowed to warm to room temperature (23 ºC) in the dark. After use, the methyl acrylate is purged with dry nitrogen and stored again in the dark at -4 ºC.

3.3.3 Distillation of 2,3-dimethyl-1,3-butadiene[1]

2,3-Dimethyl-1,3-butadiene (Alfa Aesar, 98%, 25.00 mL, 18.15 g, 0.221 moles) was added to a 50 mL round bottom flask equipped with a magnetic stir bar and $NaBH_4$ (1.00 g, 0.026 moles). A short path distillation apparatus is attached to the round bottom flask and the flask is placed in an oil bath set to 50 ºC. The fractional distillation is carried out under reduced pressure (via a Schlenk line 0.2 to 0.01 mmHg). After distillation, the diene is split into 2 portions and stored in two 20 mL oven dried glass vials at -4 ºC when not in use. Before use, the 2,3-dimethyl-1,3-butadiene is allowed to warm to room temperature (23 ºC). After use, the 2,3-dimethyl-1,3-butadiene is purged with dried nitrogen and stored in a freezer at -4 ºC.

3.4 Synthesis of reagents

3.4.1 Activation of Zn[2]

Zn (15.00 grams, 0.229 moles) was placed in a 250 mL beaker charged with a magnetic stir bar. HCl (2.00 M, 25 mL) was added to the beaker and the mixture was allowed to stir for 25 min. The stirring was stopped, and the liquid was decanted out of the beaker. The contents of the beaker was then washed with distilled water (20 mL portions, 3 times). Following the addition of each portion of distilled water, the mixture was stirred for 5 min, and the water is decanted off. The solution was then washed with acetone (20 mL portions, 3 times), and the acetone is decanted off. The Zn is then placed in a 50 mL round bottom flask stoppered with a flow control valve. The Zn is then dried under vacuum (via a Schlenk line 0.2 to 0.01 mmHg) while in an oil bath at 100 ^{o}C. The flask was then filled with argon and brought into a glove-box. The zinc was then ground into a fine powder using a ceramic mortar and pestle. The resulting activated Zn powder is stored in a 20 mL oven dried glass vial in the glove-box.

3.4.2 Synthesis of (dppp)$CoBr_2$[2]

In a glove-box, anhydrous $Co(II)Br_2$ (3.46 grams, 0.0159 moles, 1.00 eq) is added to a 250 mL round bottom flask equipped with a magnetic stir bar. In a separate 250 mL round bottom flask is taken 1,3-bis(diphenylphosphino)propane (DPPP) (6.86 grams, 0.0166 moles, 1.04 eq) with a magnetic stir bar. To the flask containing the $Co(II)Br_2$, freshly distilled THF (100 mL) is added, and the mixture is allowed to stir until all the Co(II)Br is dissolved. To the flask containing the DPPP, a minimal amount of distilled THF (20 mL) is added, and the mixture is stirred until the majority of the dppp has dissolved. The stirring is stopped for the DPPP flask and the undissolved DPPP is allowed to settle to the bottom of the flask. The dissolved DPPP solution is slowly added to the stirring $Co(II)Br_2$ solution, the undissolved DPPP is dissolved in

THF (5 mL), and the remainder of the solution is slowly added to the Co(II)Br_2 solution. The DPPP and Co(II)Br_2 solution is allowed to stir in the glove-box for 12 hr. The stirring is then stopped, and freshly distilled hexanes/diethyl ether solution (1:1 by volume, 100 mL) was added to the solution. Immediate precipitation of the (DPPP)Co(II)Br_2 complex was observed and the solution is allowed to stir for 5 min. The supernatant is then decanted to obtain a green mixture. The solution is allowed to sit undisturbed for 5 min. The mixture is then washed with diethyl ether (50 mL portions, 3 times), and the supernatant is decanted. The solid is then taken out of the box and put on a Schlenk line where it is dried via vacuum (0.2 to 0.01 mmHg) for 12 h. A green solid is obtained. The solid is then brought into the glove-box and made into a fine powder and is further dried via vacuum for an additional 12 hr. The yield of (DPPP)Co(II)Br_2 is 5.6 grams, 0.00887 moles, 56%. The (DPPP)Co(II)Br_2 is stored in the glove-box.

3.4.3 Synthesis of cationic cobalt complex

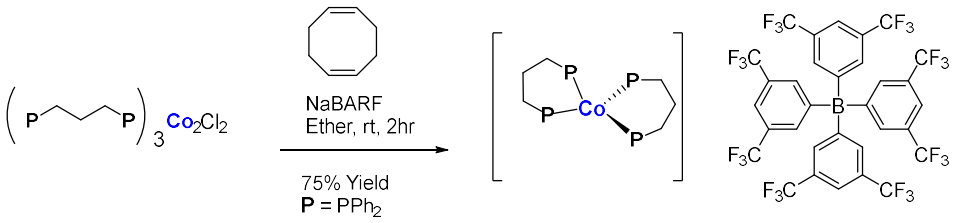

Figure 18. Procedure for synthesizing the crystalline $Co(I)^+$ $BArF^-$ complex.

In the dry-box, an 8-mL vial was charged with a magnetic stir bar, recrystallized $dppp_3Co_2Cl_2$ (50 mg, 0.035 mmol, 1 equiv.) and NaBArF (62.2 mg, 0.07 mmol, 2 equiv.).[3] The vail was capped and a solution of cyclooctadiene (COD) (0.25 mL, 1.75 mmol, 50 equiv.) in ether (5 mL) was added via syringe. The resulting green mixture was stirred for 2 hr. Upon which the color changed from green to sea green. Stirring was stopped and solvent was evacuated under high

vacuum (~0.1 mm Hg) for 2-3 h to afford crude solid. The crude solid thus obtained was then dissolved in minimum amount of ether and filtered inside the drybox. To the filtrate was then diffused hexanes (by slow evaporation of hexane into an ether solution placed in an atmosphere of hexane) to afford the sea green crystals (23 mg, 75% yield upon recrystalization). The sea green crystal was then characterized by X-ray Crystallography and the data deposited at the Cambridge Crystallographic Data Center (CCDC #1945796).

3.5 General procedure for in situ experiment

3.5.1 React IR set up

The ReactIR 45m (from Mettler Toledo) was filled with liquid N_2 and allowed to cool down for 1 h before use. The probe was attached, and the instrument was tuned to obtain optimal S/N. The readings were set to take one every 30 sec for a total of 8 hr. The instrument had the following specifications: ReactIR 45m; SN: 23553; Detector: MCT; Apodization: HappGenzel; Probe: DiComp (Diamond); SN: 23563; Interface: AgX 9.5mm x 1.5m Fiber (Silver Halide); Sampling: 3000 to 650 cm^{-1}; Resolution: 4; Scan option: AutoSelect; Gain: 1x.

3.5.2 Catalyst preparation

Before use, the glassware (see below) was cooled in a desiccator to room temperature (23 ^oC), it was then pumped into the glove-box. To a modified Schlenk flask, Figure 19, a flow control switch and a magnetic stir bar were added. Using an analytical balance (dppp)$CoBr_2$ (the indicated amounts as seen in section **5.1**), Zn dust (the indicated amounts as seen in section **5.1**), and $ZnBr_2$ (the indicated amounts as seen in section **5.1**) were weighed out and placed in the modified Schlenk flask. After the solid reagents had been added, the flask was then sealed via a

septum and electrical tape. Once sealed, the flask is taken out of the glove-box and immediately attached to a Schlenk line.

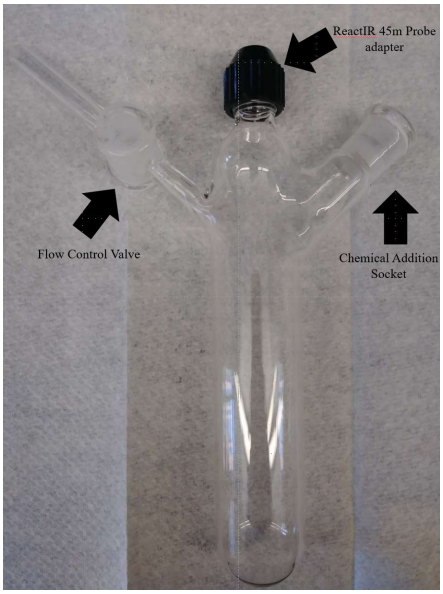

Figure 19. Modified Schlenk flask used for all procedures involving React IR.

3.5.3 Reaction set-up and analysis

The Schlenk flask attached to a Schlenk line was placed in a water bath set to 30 ºC with a stirring rate of 250 to 400 rpm. The Schlenk line was evacuated to 0.2 mmHg, and then filled with argon. This process was repeated two more times. After the line had been evacuated, the flask was open to the Schlenk line while under high argon flow. The flask itself was then evacuated to 0.2 mmHg and then filled with argon until it was at atmospheric pressure. This process was repeated 2 more times. After the third evacuation, the argon flow was turned on high, and the septa closing the top valve of the flask was removed and the ReactIR probe was placed into the neck and slid down until the tip of the probe is about 1 cm from the bottom of the flask. The probe was then sealed on and the flask was evacuated to 0.2 mmHg and then filled with argon. This process was repeated two more times for a total of three evacuations. A

background scan (180 total scans) was performed while the probe was in the flask under argon. After the scan, DCE (2 mL) was added to the flask via a 3 mL syringe and a 6 inch needle. The solution was allowed to stir for 2 hr. A color change from blue/green to red/brown was observed after about 45 min of stirring. The solution was allowed to stir for 2 h under argon. A DCE (3 mL) solution of the indicated amounts as seen in section **5.1** of methyl acrylate, 2,3-dimethyl-1,3-butadiene, and dodecane (10 μL) was prepared by adding 3 mL of distilled DCE via a 10 mL syringe, 10 uL dodecane via a 10 μL syringe, methyl acrylate via a 100 μL syringe, and 2,3-dimethyl-1,3-butadiene via a 100 μL syringe. The vial was then wrapped in aluminum foil and stored at -4 ^{o}C and taken out 30 min prior to addition in order to allow it to warm to room temperature. After the solution of (dppp)$CoBr_2$, Zn, and $ZnBr_2$ had been stirring for 2 hr, 2 mL of the solution containg methyl acrylate and 2,3-dimethyl-1,3-butadiene was added to the solution via a 3 mL syringe and disposable needle. An immediate color change from red/brown to dark green was observed upon the addition of the solution. The solution was allowed to stir for an additional 2 h after the addition of the starting material solution. The remaining 1 mL of the 3 mL starting material solution was diluted using 1 mL adding 50:50 diethyl ether:hexane mixture. The resulting solution was used to obtain a GC spectra. After 2 hr, the reaction was stopped by using a 50:50 solution of diethyl ether:hexanes (4 mL) to the reaction vessel. The resulting solution was filtered through a short pad of silica gel using an additional 4 to 8 mL of the 50:50 diethyl ether:hexane mixture to rinse the reaction vessel. A small sample was then run on the GC to analyze the conversion of diene to product. This analysis is done by comparing the ratio of the diene peak area to that of the internal standard dodecane peak of the end reaction with the ratio of the starting material mixture, Equation S1.

$$Percent\ Conversion\ of\ Diene = 1 - \frac{Diene_{Post\ Area}/Dodecane_{Post\ Area}}{Diene_{Pre\ Area}/Dodecane_{Pre\ Area}} * 100$$

Equation 21. Equation used to calculate conversion of diene via G.C. analysis.

3.5.4 IR Analysis

A ReactIR probe was used to collect in-situ data on the reaction progress and provided an infra-red spectrum every 30 sec and records the wavenumbers from 3000 cm^{-1} to 650 cm^{-1}. The peaks that are monitored for this reaction are as follows: for the methyl acrylate, 1401 cm^{-1}, for the 2,3-dimethyl-1,3-butadiene, 896 cm^{-1}, and for the product, 896 cm^{-1}.[4,5,6] The resulting data was then converted to an excel file and a MATLAB script was run that was able to fit the experimental data to a curve, using the provided curve fitting functions. After which the data was deconvoluted to put it into its final form for analysis.

3.6 Specifics for IR experiments:

3.6.1 Same Excess

Table 4. The general procedure is followed for these experiments with the following modifications

Excess Experiment	Diene (mg)	Diene (M)	Acrylate (mg)	Acrylate (M)	(dppp)$CoBr_2$ (mg)	(dppp)$CoBr_2$ (mmol)	Zn (mg)	Zn (mmol)	$ZnBr_2$ (mg)	$ZnBr_2$ (mmol)	Diene Conversion (%)[a]
Same Excess #1	32.9	0.100	89.5	0.26	96.1	0.152	99.5	1.52	356.0	1.58	90
Same Excess #2	40.1	0.122	95.4	0.28	95.8	0.152	100.0	1.53	355.4	1.58	91
Same Excess #3	49.6	0.151	106.4	0.31	95.6	0.152	99.6	1.52	354.4	1.57	98
Same Excess #4	66.0	0.201	124.3	0.36	95.9	0.152	99.6	1.52	354.9	1.58	89

[a] Determined by GC-FID analysis.

3.6.2 Different Excess

Table 5. The general procedure is followed for these experiments with the following modifications

Excess Experiment	Diene (mg)	Diene (M)	Acrylate (mg)	Acrylate (M)	(dppp)$CoBr_2$ (mg)	(dppp)$CoBr_2$ (mmol)	Zn (mg)	Zn (mmol)	$ZnBr_2$ (mg)	$ZnBr_2$ (mmol)	Conversion of Diene (%)[a]
Different Excess #1	49.6	0.151	58.2	0.17	95.7	0.152	99.6	1.52	355.7	1.58	97
Different Excess #2	47.6	0.145	68.9	0.20	96.2	0.153	99.9	1.53	354.9	1.58	92
Different Excess #3	49.9	0.152	108.1	0.31	95.5	0.151	100.6	1.55	354.5	1.57	94
Different Excess #4	49.6	0.151	106.4	0.31	95.6	0.152	99.6	1.52	354.4	1.57	98

[a] Determined by GC-FID analysis.

3.6.3 Stir Test

Table 6. The general procedure is followed for these experiments with the following modifications

Stir Time for Initial Catalyst Mixture	Diene (mg)	Diene (M)	Acrylate (mg)	Acrylate (M)	(dppp)$CoBr_2$ (mg)	(dppp)$CoBr_2$ (mmol)	Zn (mg)	Zn (mmol)	$ZnBr_2$ (mg)	$ZnBr_2$ (mmol)	Conversion of Diene (%)[a]
5 min	50.3	0.153	105.7	0.307	96.0	0.152	99.9	1.53	356.5	1.58	90
30 min	50.3	0.153	105.7	0.307	96.0	0.152	99.9	1.53	356.5	1.58	90
1 hr	50.3	0.153	105.7	0.307	95.8	0.152	100.3	1.53	354.6	1.57	90
2 hr	50.3	0.153	105.7	0.307	95.8	0.152	100.5	1.54	353.8	1.57	90
8 hr	50.3	0.153	105.7	0.307	95.6	0.152	99.6	1.52	354.6	1.57	96

[a] Determined by GC-FID analysis.

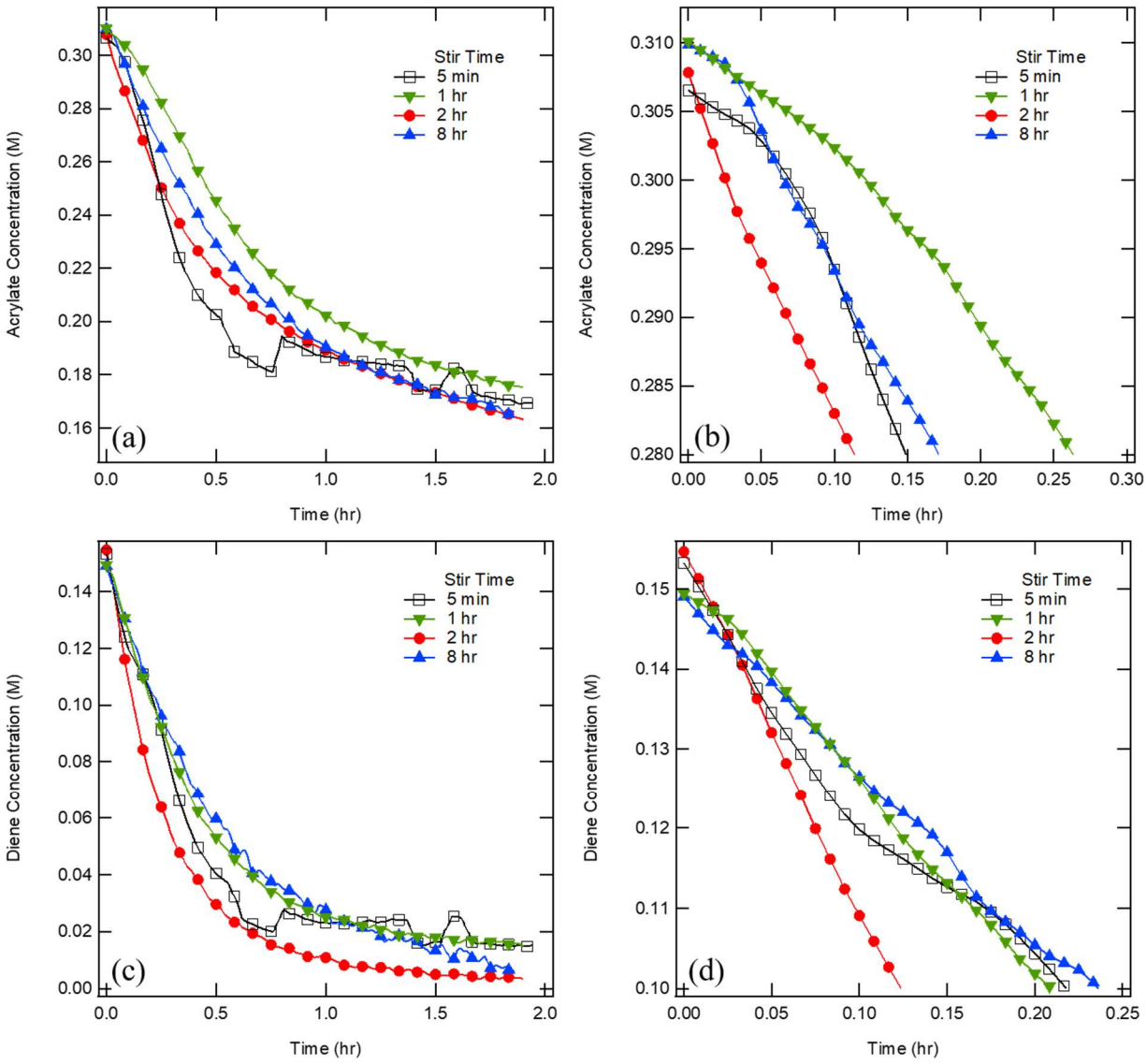

Figure 21. (a) Acrylate concentration, measured by the intensity at 1401 cm^{-1}, vs time for stir time investigations at 5 min, 1 hour, 2 hours, and 8 hours. Insert shows a zoomed in region of the first 18 minutes of the reaction. The data shown only shows 1 in every 10 data points collected for clarity of the figure. (b) Zoomed in region of (a) shows time from 0 to 0.21 hours. Data points are not sparse. (c) Diene concentration, measured by the intensity at 896 cm^{-1}, vs. time for stir time investigations at 5 min, 1 hour, 2 hours, and 8 hours. Insert shows a zoomed in region of the first 18 minutes of the reaction. The data shown only shows 1 in every 10 data points collected for clarity of the figure. (d) Zoomed in region of (b) shows time from 0 to 0.25 hours. Data points are not sparse.

3.6.4 Catalyst Order Test

Table 7. The general procedure is followed for these experiments with the following modifications

Catalyst Loading	Diene (mg)	Diene (M)	Acrylate (mg)	Acrylate (M)	(dppp)$CoBr_2$ (mg)	(dppp)$CoBr_2$ (mmol)	Zn (mg)	Zn (mmol)	$ZnBr_2$ (mg)	$ZnBr_2$ (mmol)	Conversion of Diene (%)
Normal	49.9	0.152	107.4	0.312	95.5	0.151	100.6	1.54	354.5	1.574	94
Half Catalyst Loading	49.6	0.151	107.8	0.313	47.9	0.076	50.5	0.77	178.7	0.794	98
Three Thirds Catalyst Loading	49.6	0.151	110.2	0.320	74.9	0.119	77.8	1.20	266.4	1.18	> 99

[a] Determined by GC-FID analysis.

3.6.5 Diene polymerization without catalyst Test

The general procedure is followed for these experiments with the following modifications

1. Diene amount: 0.152 M
2. Acrylate amount: 0.00
3. (dppp)$CoBr_2$ amount: 0
4. Zn amount: 0
5. $ZnBr_2$: 0
6. DCE used: 4 mL
7. Ligand amount: 0.00
8. Conversion: 0%

3.6.6 Diene polymerization with catalyst Test

The general procedure was followed for these experiments with the following modifications

1. Diene amount: 0.148 M

2. Acrylate amount: 0.00
3. (dppp)$CoBr_2$ amount: 0.151 mmol
4. Zn amount: 1.50 mmol
5. $ZnBr_2$: 1.55 mmol
6. DCE used: 4 mL
7. Ligand amount: 0.00
8. Conversion: 20%

3.7 Isotopic Labeling Experiments

3.7.1 Reversibility of β-hydride elimination

Inside a glove-box, to an oven-dried 8 mL screw cap vial equipped with a stir bar and screw septum cap, (DPPP)Co(II)Br_2 (10.2 mg, 0.016 mmol), Zn (9.5 mg, 0.15 mmol), and $ZnBr_2$ (32.4 mg, 0.144 mmol) were added. Upon the starting of stirring, DCM (1 mL); stored with molecular sieves, was added to the vial. The solution was allowed to stir undisturbed for 2 hr. After the 2 hour period, methyl acrylate-d_3 (23.3 mg, 0.26 mmol) was added neat the solution via a 100 µL syringe. Directly after this addition 2,3-dimethyl-1,3-butadiene (20.3 mg, 0.25 mmol) was added to the solution via a 100 µL syringe. The reaction was allowed to react for three hr. After which the reaction was stopped with a 1:1 solution by volume of diethyl ether and pentanes. The reaction was purified by evaporating off all the solvents and starting materials to yield pure deuterated product (17.00 mg, 0. 099 mmol, 39.6 %yield)**.**

3.8 Co(I) activity vs $Co(I)^+$ activity

Inside a glove-box, to an oven dried 8 mL screw cap vial equipped with a stir bar and screw septum cap, (DPPP)3Co_2(I)Br_2 (5.5 mg, 0.009 mmol) was added. DCM (0.5 mL), that was

stored with molecular sieves, was added to the vial. The solution was allowed to stir for 2 hr, after which, methyl acrylate (17.2 mg, 0.20 mmol) and 2,3-dimethyl-1,3-butadiene (14.5 mg, 0.18 mmol) in 0.5 mL DCM was added. The reaction was allowed to proceed for 2 hr. The reaction was then stopped with a 1:1 solution of diethyl ether and hexanes. The progress was monitored via gas chromatography. The G.C. showed no product formation. In a parallel reaction inside a glove-box, to an oven dried 8 mL screw cap vial equipped with a stir bar and screw septum cap, $(DPPP)_3Co_2(I)Br_2$ (6.6 mg, 0.01 mmol) and $ZnBr_2$ (32.2 mg, 0.143 mmol) was added. DCM (0.5 mL), that was stored with molecular sieves, was added to the vial. The solution was allowed to stir for 2 hr, after which, methyl acrylate (17.2 mg, 0.20 mmol) and 2,3-dimethyl-1,3-butadiene (14.5 mg, 0.18 mmol) in 0.5 mL DCM was added. The reaction was allowed to proceed for 2 hr. The reaction was then stopped with a 1:1 solution of diethyl ether and hexanes. The progress was monitored via gas chromatography The G.C. showed 19.2% conversion of diene.

3.9 UV-Vis studies

3.9.1 Background

A background of DCE was taken. To a modified cuvette that allowed the preservation of air sensitive materials, 2 mL of freshly distilled DCE was added. The cuvette was placed in the in-situ UV-VIS and a wavelength scan was performed from 1100 nm to 190 nm. This reading was used as the background for the rest of the UV-Vis experiments.

3.9.2 $(DPPP)_3Co^{(I)}{}_2Br_2$

To a clean 4 mL oven dried glass vial, 2.2 mg of $(DPPP)_3Co(I)_2Br_2$[2] (recrystallized from THF upon diffusion with hexanes) and DCE (2 mL) were added to the vial. While in a glove-

box, the solution was transferred to a modified cuvette. The cuvette was taken out of the glove-box and placed in the in-situ UV-Vis and a wavelength scan from 1100 nm to 190 nm was performed.

3.9.3 (DPPP)$Co^{(II)}Br_2$

To a clean 4 mL oven dried glass vial, 2.5 mg of (DPPP)$Co^{(II)}Br_2$ and DCE (2 mL) were added to the vial. While in a glove-box, the solution was transferred to a modified cuvette. The cuvette was taken out of the glove-box and placed in the in-situ UV-VIS and a wavelength scan from 1100 nm to 190 nm was performed.

3.9.4 $[(DPPP)Co^{(I)}]^+$

While inside a glove-box, to a clean 20 mL oven dried glass vial, a magnetic stir bar, (dppp)$Co^{(II)}Br_2$ (48.00 mg, 0.0761 mmols, 1 eq), activate Zn dust (49.00 mg, 0.778 mmols, 10.22 eq) and $ZnBr_2$ (171.00 mg, 0.759 mmols, 9.98 eq) and DCE (2 mL) were added. The solution was allowed to stir for 2 hr inside the glove-box. After this period, the solution changed colors from a blue/green to a dark red/brown. After a 2 hour stirring period, 0.100 mL of the solution's was transferred to a modified cuvette and then DCE (1.900 mL) was added to the cuvette to make a 0.002 M solution of (DPPP)$Co(I)^+$. The cuvette was taken out of the glove-box and placed in the in-situ UV-VIS and a wavelength scan from 1100 nm to 190 nm was taken every minute for four min.

3.9.5 Diene Coordination

To a freshly prepared sample of $[(DPPP)Co^{(I)}]^{+}$, prepared as described above at 0.002 M, 2,3-dimethyl-1,3-butadiene in DCE was added to the cuvette (0.176 molar, 0.044 mmols, 11 eq) and a wavelength scan from 1100 nm to 190 nm was taken every minute for five min.

3.9.6 Acrylate Coordination

To a freshly prepared sample of $[(DPPP)Co^{(I)}]^{+}$, prepared as described above at 0.002 M, methyl acrylate in DCE was added to the cuvette (0.464 molar, 0.232 mmols, 58 eq) and a wavelength scan from 1100 nm to 190 nm was taken every minute for four min.

3.9.7 Diene vs Acrylate Competition Test

To a freshly prepared sample of $[(DPPP)Co^{(I)}]^{+}$, prepared as described above at 0.002 M, methyl acrylate in DCE was added to the cuvette (0.464 molar, 0.232 mmols, 58 eq) and a wavelength scan from 1100 nm to 190 nm was taken every minute for four min. After this, 2,3-dimethyl-1,3-butadiene in DCE was added to the cuvette (0.176 molar, 0.044 mmols, 11 eq) and a wavelength scan from 1100 nm to 190 nm was taken every minute for five min.

3.9.8 Synthesis and UV-Vis Analysis of Cationic Cobalt(I) from $(DPPP)_3Co_2^{(I)}Br_2$ crystal.

To a modified cuvette, crystalline $(DPPP)_3Co_2{}^{(I)}Br_2$ (3.4 mg, 0.002 mmole) and NaBArF (3.9 mg, 0.004 mmole), and 2 mL of DCE were added. The solution was allowed to stir for 15 min after which, UV-Vis spectra was recorded with a wavelength scan from 1100 nm to 190 nm.

3.9.9 Stir Time Analysis UV-Vis

While inside a glove-box, to a clean 20 mL oven dried glass vial, a magnetic stir bar, $(DPPP)Co^{(II)}Br_2$ (19.80 mg, 0.031 mmols, 1 eq), activate Zn dust (20.3 mg, 0.31 mmols, 10.00 eq) and $ZnBr_2$ (70.00 mg, 0.31 mmols, 10.00 eq) and DCE (2 mL) were added. The solution was

allowed to stir for 2 hr inside the glove-box. After this period, the solution changed colors from a blue/green to a dark red/brown. After a 120 min, 150 min, 240 min, and 270 min stirring period, 0.050 mL of the solution was transferred to a modified cuvette and then DCE (1.950 mL) was added to the cuvette to make a 0.002 M solution of (dppp)Co(I)$^{+}$. The cuvette was taken out of the glove-box and placed in the in-situ UV-VIS and a wavelength scan from 1100 nm to 190 nm was taken. The UV-Vis reading was performed.

3.10 Reaction Engineering

3.10.1 High Concentration Batch Reaction

While inside a glove-box, to an oven dried 50.00 mL Schlenk flask was charged with a magnetic stir bar, (DPPP)$CoBr_2$ (96.2 mg, 0.152 mmol, 0.01 eq), Zn (95.8 mg, 1.47 mmol, 0.1 eq), and $ZnBr_2$ (345 mg, 1.53 mmol, 0.1 eq). The flask was then taken and attached to a Schlenk line. Once on the Schlenk line, the flask was evacuated to 0.2 mmHg, and then filled with argon. This process was repeated 2 more times. After the line has been evacuated, the Schlenk flask was open to the Schlenk line while under high argon flow. The flask itself was then evacuated to 0.2 mmHg and then filled with argon until it was at atmospheric pressure. This process was repeated 2 more times. To the flask DCE was added (2 mL) and the mixture was allowed to stir for 2 hr. After the 2 hr, methyl acrylate (1.6 mL, 17.8 mmol, 1.1 eq), 2,3-dimethyl-1,3-butadiene (1.8 mL, 15.9 mmol, 1.0 eq), and dodecane (30 μL), as an internal standard, were added to the flask. The reaction was allowed to react for eighteen hr after which it was stopped by adding a 1:1 mixture of pentane:diethyl ether. The resulting suspension was filtered through a short pad of silica and a small aliquot was analyzed via GC-FID to yield product in 48% conversion.

3.11 Stir Time Comparison

3.11.1 Stir Time Analysis of $ZnBr_2$ vs NaBArF

To an 8 mL vial, (DPPP)$CoBr_2$ (9.5 mg, 0.015 mmole, 0.095 eq), Zn (11 mg, 0.17 mmole, 1.08 eq), and NaBArF (14.8 mg, 0.017, 0.108 eq) and a magnetic spin vane was added. To the 8 mL vial, DCM (0.50 mL) was added. The mixture was allowed to stir fir five minutes. After the 5 minute stir period, 2,3-dimethyl-1,3-butadiene (13 mg, 0.158 mmole, 1 eq), methyl acrylate (15 mg, 0.17 mmole, 1.08 eq), and DCM (0.5 mL) were added to the solution. The solution was allowed to stir for five minutes. After five minutes, the reaction progress was monitered by G.C. by taking out a small aliquot and diluting this with approximately 1 mL of 1:1 ether:hexanes mixture. The reaction was again monitered after 15 min and then again after 25 minutes. This procedure was repeated two additional times.

To an 8 mL vial, (DPPP)$CoBr_2$ (9.5 mg, 0.015 mmole, 0.095 eq), Zn (11 mg, 0.17 mmole, 1.08 eq), and $ZnBr_2$ (5.5 mg, 0.024, 0.15 eq) and a magnetic spin vane was added. To the 8 mL vial, DCM (0.50 mL) was added. The mixture was allowed to stir fir five minutes. After the 5 minute stir period, 2,3-dimethyl-1,3-butadiene (13 mg, 0.158 mmole, 1 eq), methyl acrylate (15 mg, 0.17 mmole, 1.08 eq), and DCM (0.5 mL) were added to the solution. The solution was allowed to stir for five minutes. After five minutes, the reaction progress was monitered by G.C. by taking out a small aliquot and diluting this with approximately 1 mL of 1:1 ether:hexanes mixture. The reaction was again monitered after 15 min and then again after 25 minutes. This procedure was repeated two additional times.

The results for the above test can be seen in the table below. The conversion was calculated by using an internal standard of dodecane with gas chromatography.

Table 8. Experimental parameters for the induction period.

	0 min (% conversion)	5 min (% conversion)	15 min (% conversion)	25 min (% conversion)
$ZnBr_2$ (average)	0.0 ± 0.0	0.0 ± 0.0	0.0 ± 0.0	5.3 ± 3.1
NaBArF (average)	0.0 ± 0.0	38.0 ± 7.3	70.0 ± 4.3	89.3 ± 3.3
$ZnBr_2$ (trial 1)	0.0	0.0	0.0	1.0
$ZnBr_2$ (trial 2)	0.0	0.0	0.0	7.0
$ZnBr_2$ (trial 3)	0.0	0.0	0.0	8.0
NaBArF (trial 1)	0.0	48.0	68.0	90.0
NaBArF (trial 2)	0.0	31.0	66.0	85.0
NaBArF (trial 3)	0.0	35.0	76.0	93.0

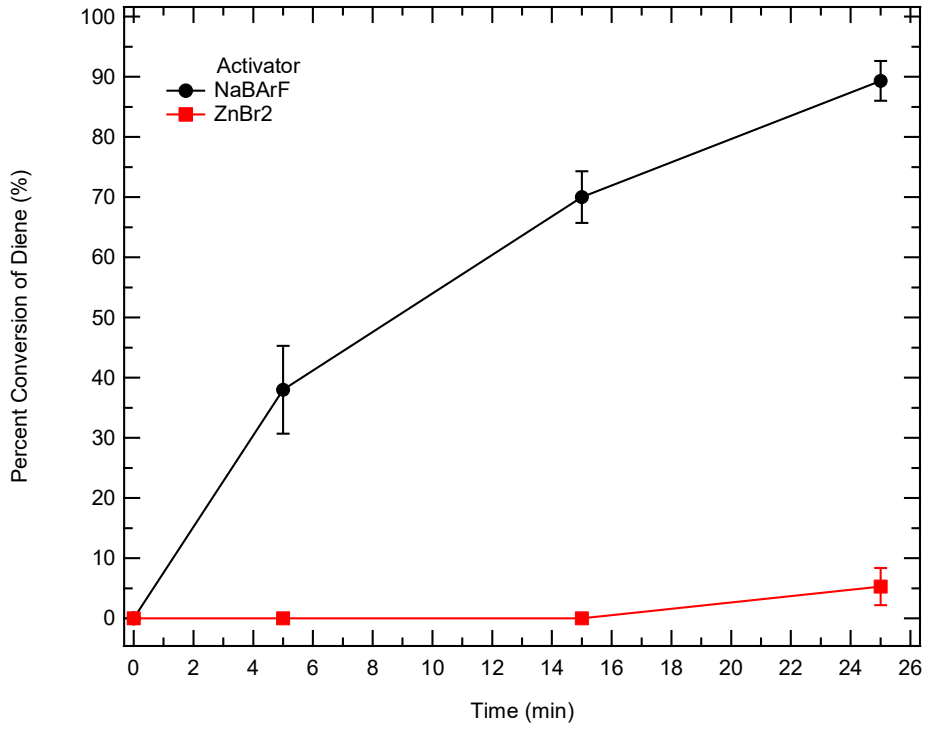

Figure 22. The average percent conversion (with standard deviation) of the test shown above. The red line represents the percent conversion using $ZnBr_2$ activation across twenty five minutes. The

black line represents the percent conversion using NaBArF activation across twenty five minutes. The percent conversions was found using gas chromatography and an internal standard of dodecane.

3.12 Spectral Analysis

3.12.1 ^{1}H and ^{13}C NMR of Pure product

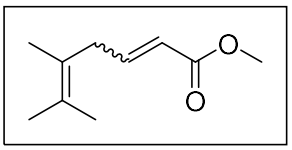

Methyl 5,6-dimethylhepta-2,5-dienoate: The reaction between 2.3-dimethyl-1,3-butadiene (145.20 mg, 1.77 mmol) and methyl acrylate (249.52, 2.90 mmol) in DCM and (dppp)$CoBr_2$ (153.00 mg, 0.24 mmol), zn (156 mg, 0.69 mmol), and $ZnBr_2$ (590 mg, 0.67 mmol) and were reacted for 4 hr. Upon completion, the reaction was filtered through a short pad of silica using 50:50 diethyl ether:hexanes (5 mL). The product was isolated by evaporating off the solvent to yield the titled compound as a colorless oil. 90% yield from G.C. analysis. ^{1}H NMR (400 MHz, $CDCl_3$): δ 6.90 (dt, , J = 15.66 Hz, 6.54, 1 H), 5.77 (dt, J = 15.46, 1.66, 1 H), 3.71 (s, 3 H), 2.89 (d, 6.60 , 2 H), 1.67 (s, 3 H), 1.63 (s, 6 H). ^{13}C NMR (400 MHz, $CDCl_3$): δ 167.58, 147.57, 127.65, 123.49, 51.69, 37.74, 20.90, 20.56, 18.94

3.12.2 NMR Analysis of (dppp)Co(m)Br_n Species

All the NMR samples were made inside the N_2- filled glove-box (Specific amount of each species is mentioned on the corresponding spectra). The NMR tube was capped which was wrapped by Teflon tape.

1. (DPPP)$CoBr_2$ (10 mg dissolved in 0.6mL $CDCl_3$ in NMR tube) – no ^{31}P Signal
2. (DPPPP)$CoBr_2$ (10 mg, 0.0158 mmol, 1 equiv.) and Zn (10 mg, 0.158 mmol, 10 equiv.) dissolved in 0.6mL $CDCl_3$ in NMR tube. NMR took after 15 min – ^{31}P (243 MHz, $CDCl_3$) δ -21.87, 15.47.

3. (DPPPP)$CoBr_2$ (10 mg, 0.0158 mmol, 1 equiv.), Zn (10 mg, 10 equiv.), and $ZnBr_2$ (7mg, 2 equiv.) dissolved in 0.6 mL $CDCl_3$ in NMR tube. ^{31}P NMR took after 30 min. ^{31}P (243 MHz, $CDCl_3$) δ -21.89 (No peak at δ ~ 15.47)

4. (DPPP)$CoBr_2$ (10 mg, 0.0158 mmol, 1 equiv.), Zn (10 mg, 10 equiv.), and NaBARF (18mg, 2 equiv.) dissolved in 0.6 mL $CDCl_3$ in NMR tube. 31P NMR took after 30 min. ^{31}P (243 MHz, $CDCl_3$) δ -21.29

3.12.3 ^{1}H and ^{13}C NMR of Deuterated product

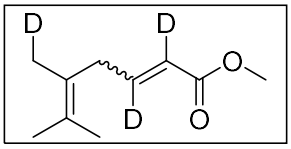

d_3-Methyl 5,6-dimethylhepta-2,5-dienoate: The reaction between 2.3-dimethyl-1,3-butadiene (20.3 mg, 0.25 mmol) and d_3-methyl acrylate (23.3 mg, 0.26 mmol) in DCM and (dppp)$CoBr_2$ ((10.2 mg, 0.016 mmol), Zn (9.5 mg, 0.15 mmol), and $ZnBr_2$ (32.4 mg, 0.144 mmol) and were reacted for 3 hr. Upon completion, the reaction was filtered through a short pad of silica using 50:50 diethyl ether:pentanes (5 mL). The product was isolated by evaporating off the solvent to yield the titled compound as a colorless oil. 39.6 % yield by G.C. ^{1}H NMR (600 MHz, $CDCl_3$): δ 3.71 (s, 3 H), 2.89 (s, 2 H), 1.67 (s, 3 H), 1.63 (s, 6 H). ^{13}C NMR (600 MHz, $CDCl_3$): δ 167.42, 147.57, 127.44, 123.32, 51.508, 37.4203, 20.70, 20.1 (t, 19.5 Hz, CDH_2), 18.75

3.13 ^{1}H and ^{13}C NMR and Chromatograms

3.14 Refernces

(1) Perrin, D. D. Armarego, W. L. F. and Perrin, D. R. Purification of Laboratory Chemicals, 2nd ed.; Pergamon Press: 1980

(2) Jing, S. M.; Balasanthiran, V.; Pagar, V.; Gallucci, J. C.; RajanBabu, T. V. Catalytic Enantioselective Hetero-dimerization of Acrylates and 1,3-Dienes. *J. Am. Chem. Soc.* **2017**, *139*, 18034-18043.

(3) Duvvuri, K.; Dewese, K. R.; Parsutkar, M. M.; Jing, S. M.; Mehta, M.; RajanBabu, T. V. Cationic Co(I)-Intermediates for Hydrofunctionalization reactions: Regio- and Enatioselective Cobalt-Catalyzed 1,2-Hydroboration of 1,3-Dienes. *J. Am. Chem. Soc.* **2019**, 141, 7365-7375.

(4) SDBSWeb : https://sdbs.db.aist.go.jp (National Institute of Advanced Industrial Science and Technology, May 1st 2019)

(5) Carmona, P.; Moreno, J. The infrared spectra and structure of methyl acrylate. *J. Mol. Struct.* **1982**, *82*, 177-185.

(6) Durig, J. R.; Compton, D. A. C. Analysis of torsional spectra of molecules with 2 internal C3v rotors. 16. Infrared and Raman spectra, vibrational assignment, methyl torsional potential function, and gas phase thermodynamic functions of 2,3-dimethylbuta-1,3-dien. *J. Phys. Chem.* **1979**, *83*, 2879-2886.

(7) Kryzystek, J.; Ozarowski, A.; Zvyagin, S. A.; Tesler, J. High Spin Co(I): High-Frequency and –Field EPR Spectroscopy of $CoX(PPh_3)_3$. *Inorg. Chem.* **2012**, 51, 4954-4964.

(8) Sacconi, L.; Midollini, S. Halogeno-Complexes of Cobalt(I) and Nickel(I) with 1,1,1-tris(diphenyl-phosphinomethyl)ethane. *J.C.S. Dalton.* **1972**, 1213-1216.

(9) Rose, M. J.; Bellone, D. E.; Di Bilio, A. J.; Gray, H. B. Spectroscopic and Magnetic Properties of an Iodo Co^I Tripodal Phosphine Complex. *Dalton Trans.* **2012**, 41, 11788-11797.

(10) Aresta, M.; Rossi, M; Sacco, A. Tetrahedral Complexes of Cobalt(I). *Inorganica Chimica Acta.* **1969**, 227-231.

(11) Kiefer, G.; Vrubel, H.; Scopelliti, R.; Severin, K. The Intricate Chemistry of Cobalt(II) Halides and Bis(diphenylphosphanyl)ethane. *Eur. J. Inorg. Chem.* **2013**, 4619-4921.